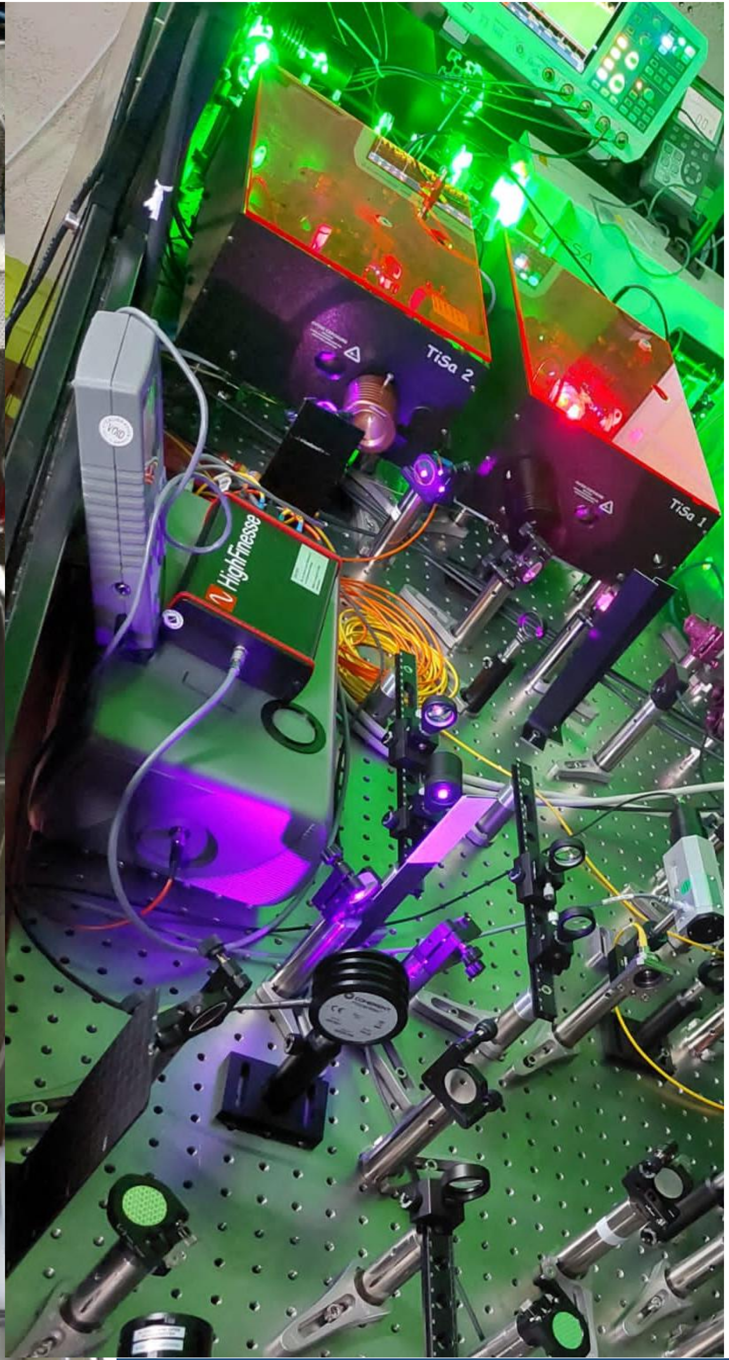

Optimization of in-gas-jet laser spectroscopy with S^3-LEB

Anjali Ajayakumar

LISA_ITN / GANIL

laboratoire commun CEA/DRF CNRS/IN2P3

Outline

- S^3-LEB set up
- IGLIS method
- Offline commissioning tests and results
- Conclusion and outlook

GANIL- SPIRAL2 facility

- Aim to deliver high intensity primary beams from H to U (>1pμA)
- Delivery of beam to NFS in operation
- S^3 : Nuclear fusion evaporation to produce exotic nuclei.

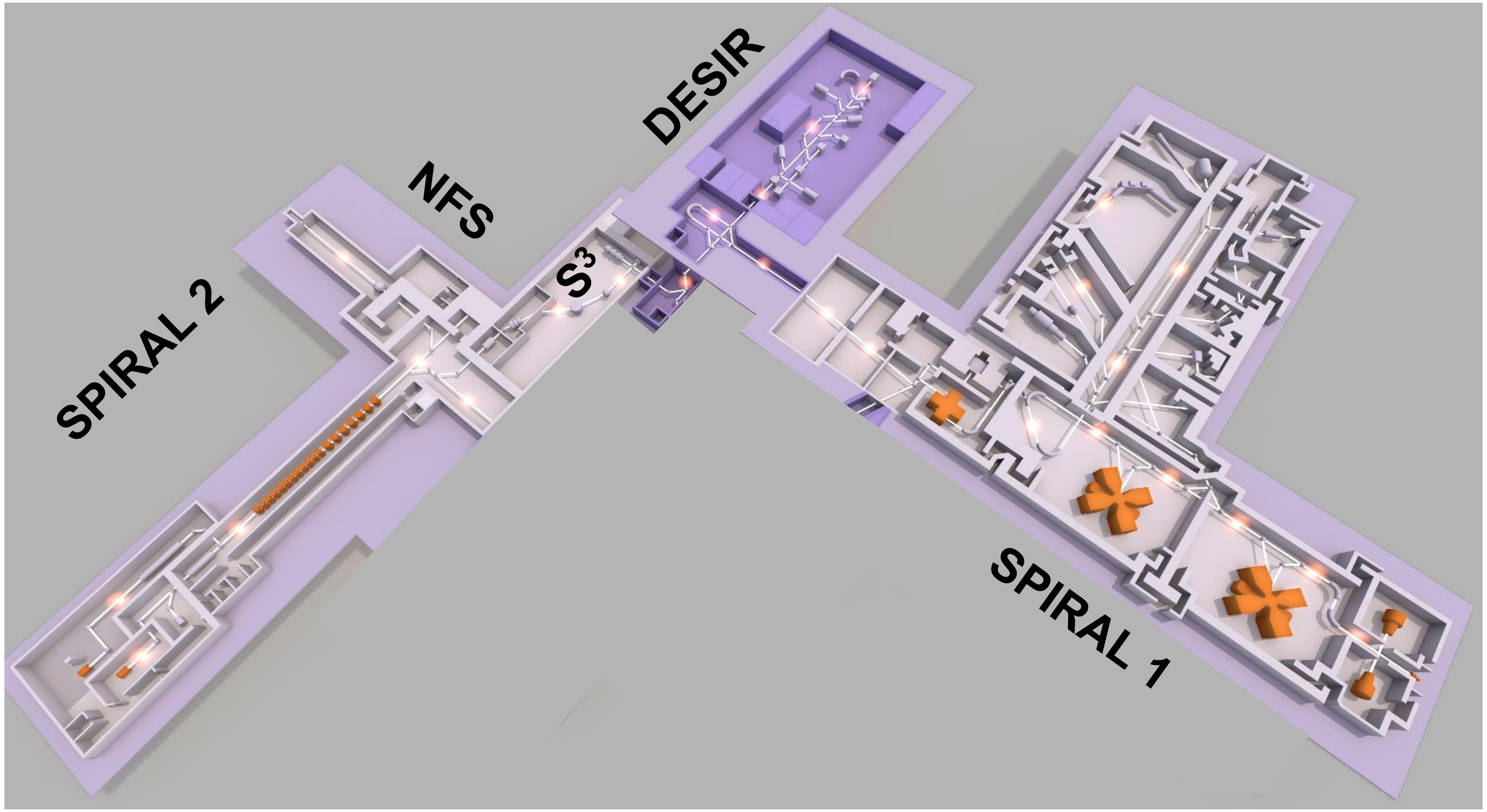

Super Separator Spectrometer (S^3)

- High resolution Recoil separator
- Primary beam rejection and high acceptance
- Mass resolution >450
- T> 50 %

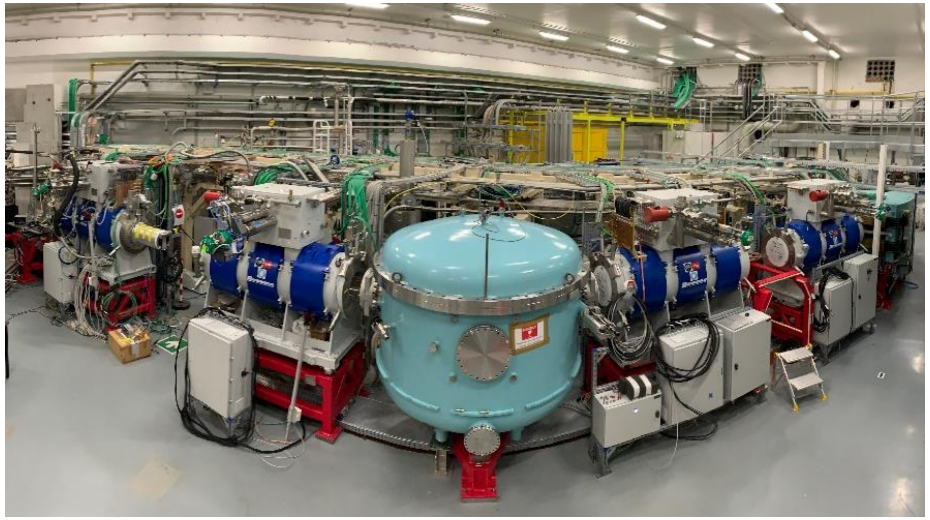

S^3 in the finishing stages

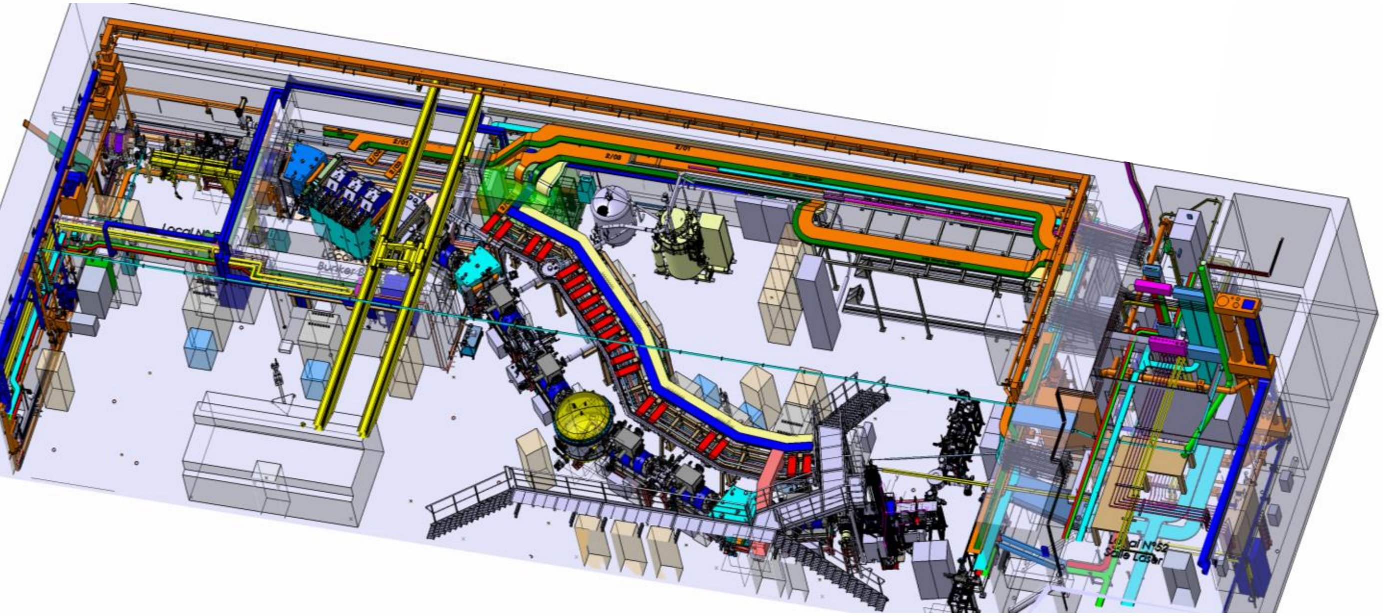

Low energy branch
- At the focal plane of S^3

Super Separator Spectrometer Low Energy Branch (S^3-LEB)

laboratoire commun CEA/DRF CNRS/IN2P3

- **Laser spectroscopy**
- Mass spectrometry
- Decay spectroscopy

In-gas laser ionization and spectroscopy (IGLIS)

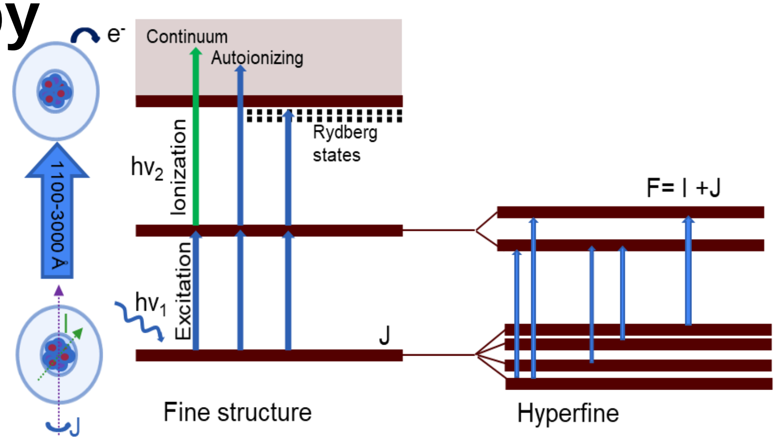

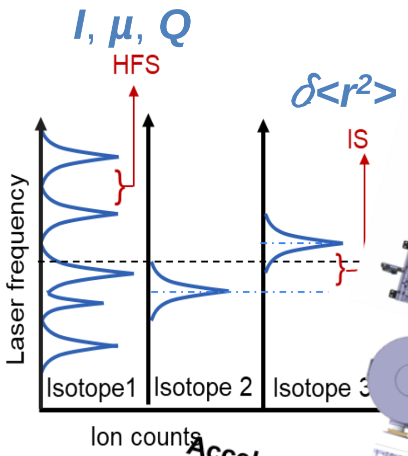

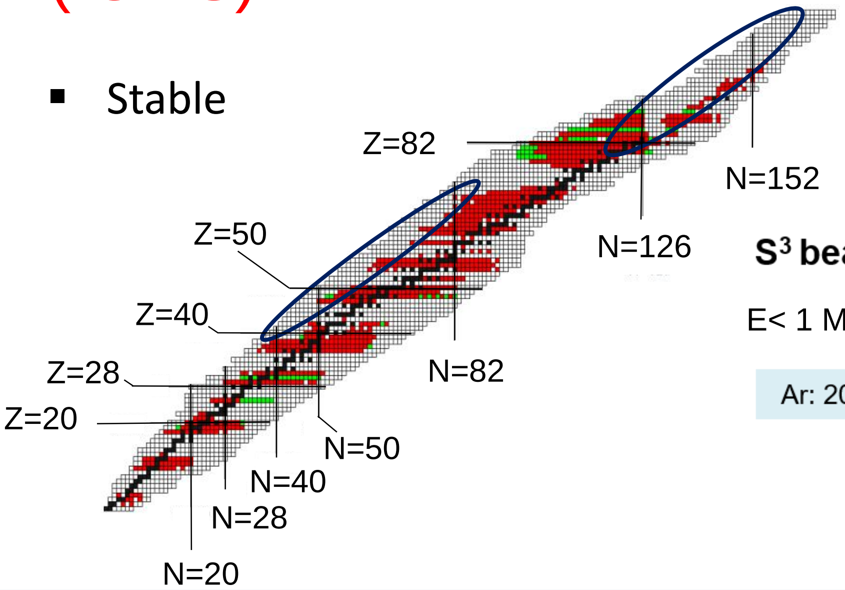

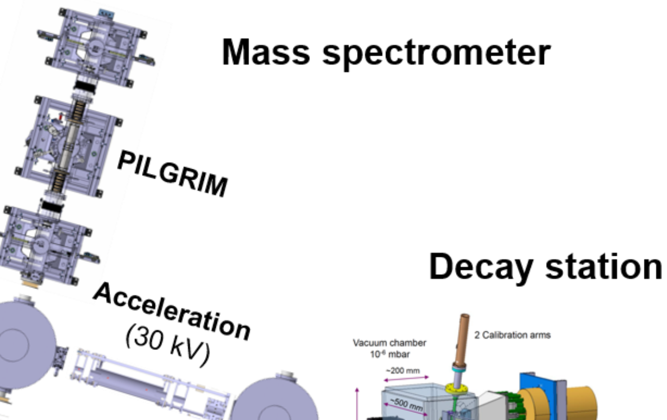

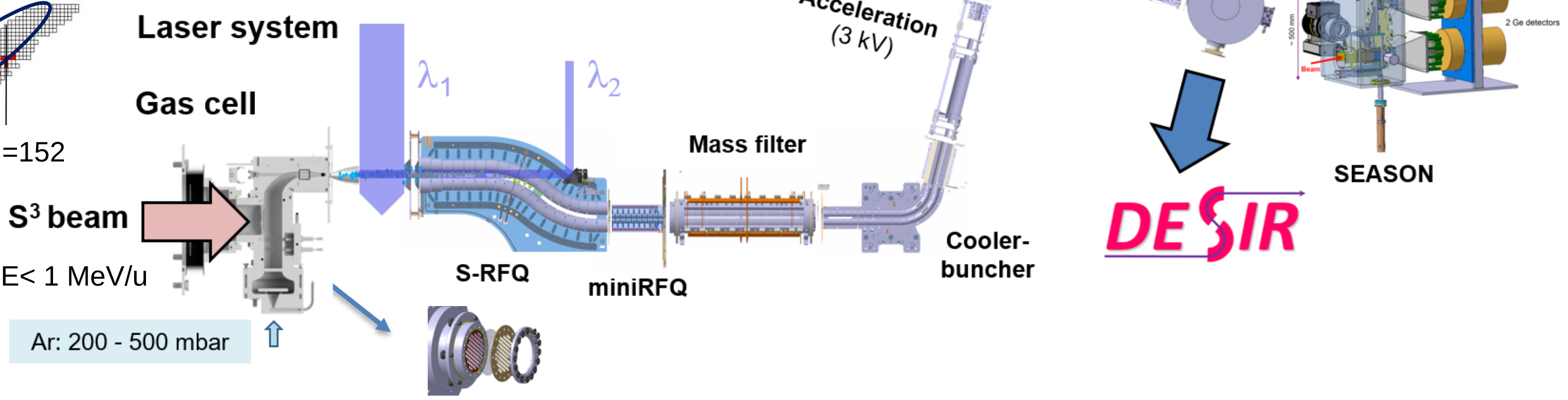

R. Ferrer et al., Nucl. Instr. Meth. B 317, 570-581 (2013)
J. Romans, et al., Atoms 10, 21 (2022)
A. Ajayakumar et al., Nucl. Instr. Meth. B 539, 102-107 (2023)

IGLIS method

Gas cell

- Broadening effects
- Broad band laser (GHz)

de Laval nozzle

- Hypersonic gas jet:

  ρ ↓ & T ↓

- Narrow band laser (MHz)

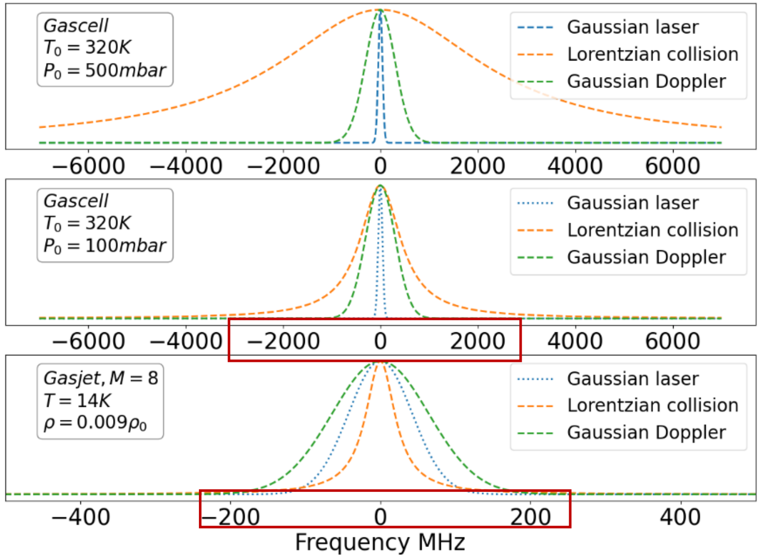

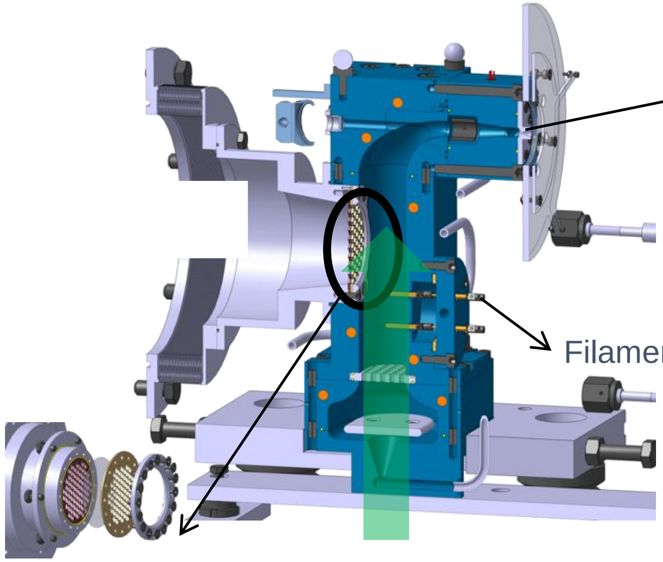

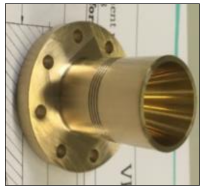

de Laval nozzle

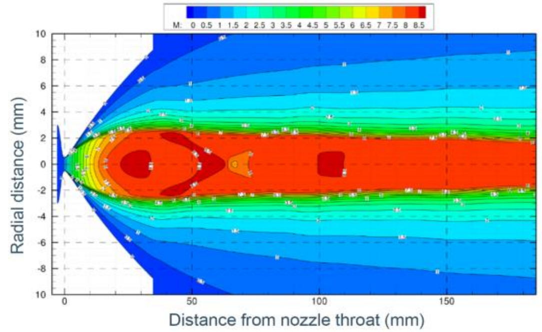

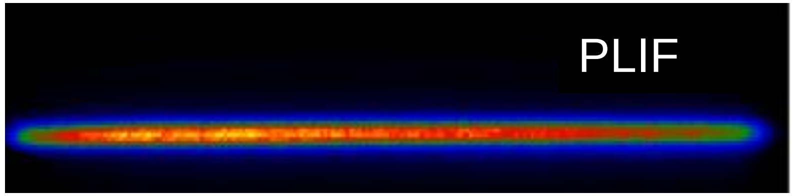

A. Zadvornaya et al. Phy.Rev X 8 041008 (2018)

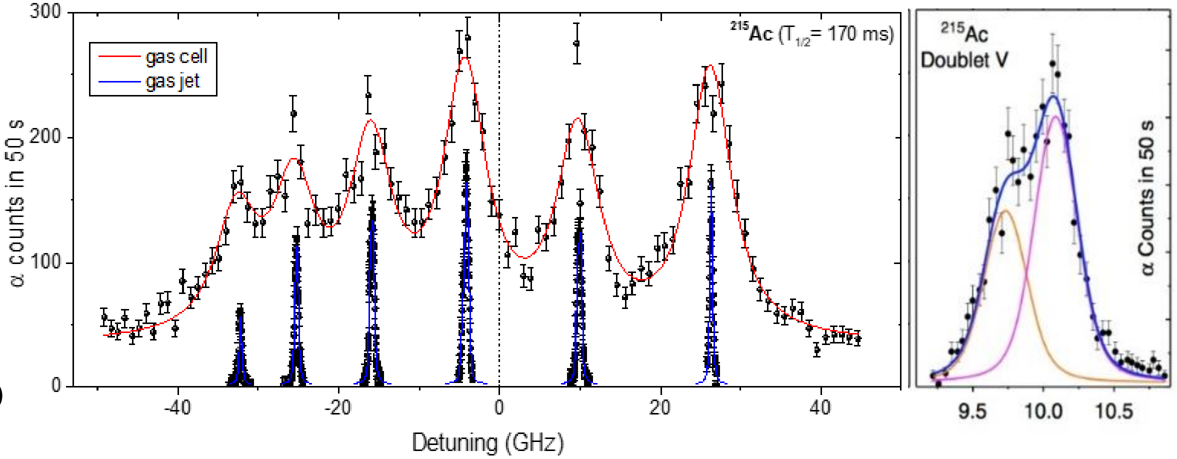

R. Ferrer et al. Phy Rev Res 3, 043041 (2021)

R. Ferrer et al. Nat. Comm..8.14520 (2017)

OFFLINE commissioning results

- Er Resonance laser ionization
  - First case for S^3-LEB
- In gas cell/gas jet laser spectroscopy
- Isotope detection by PILGRIM

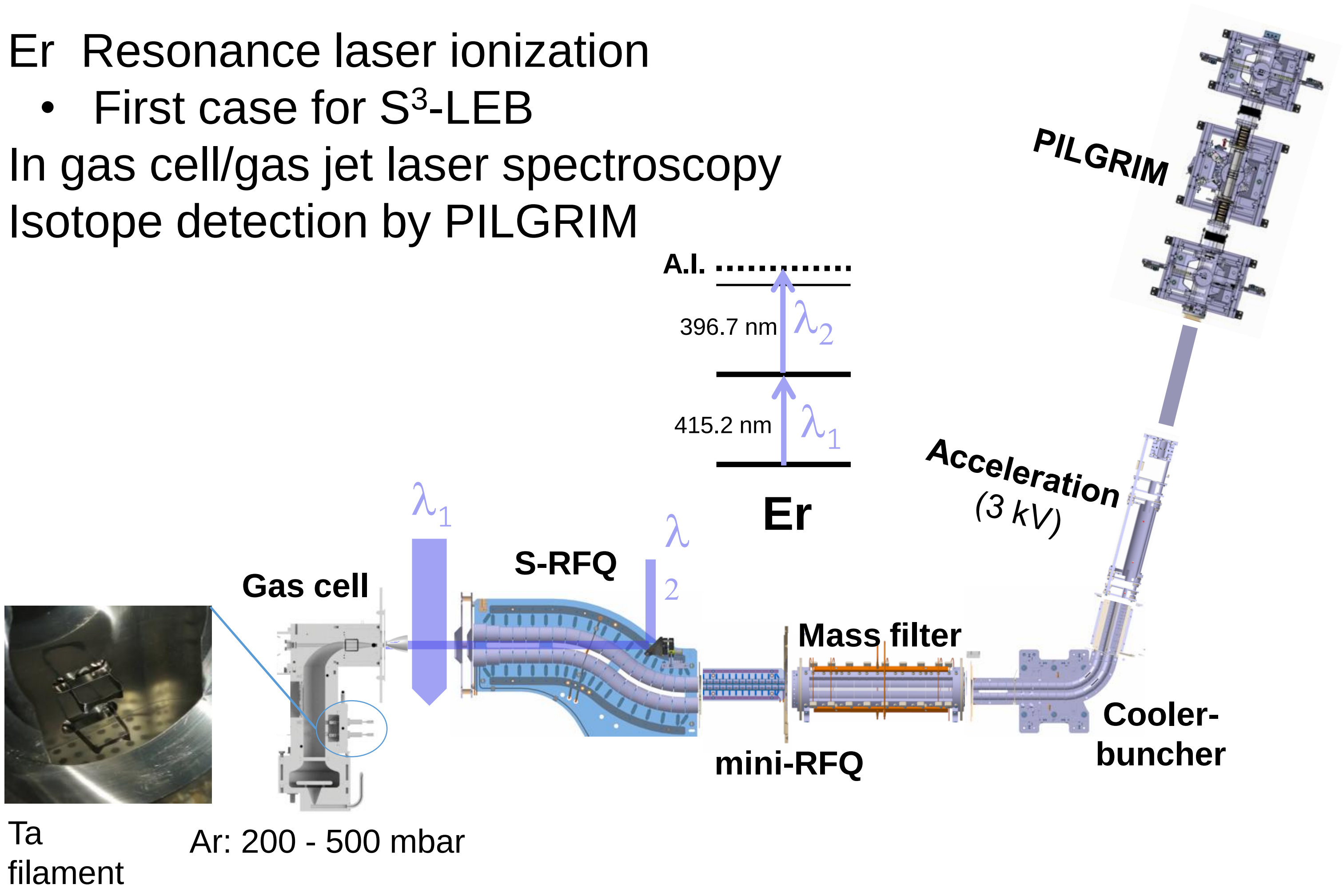

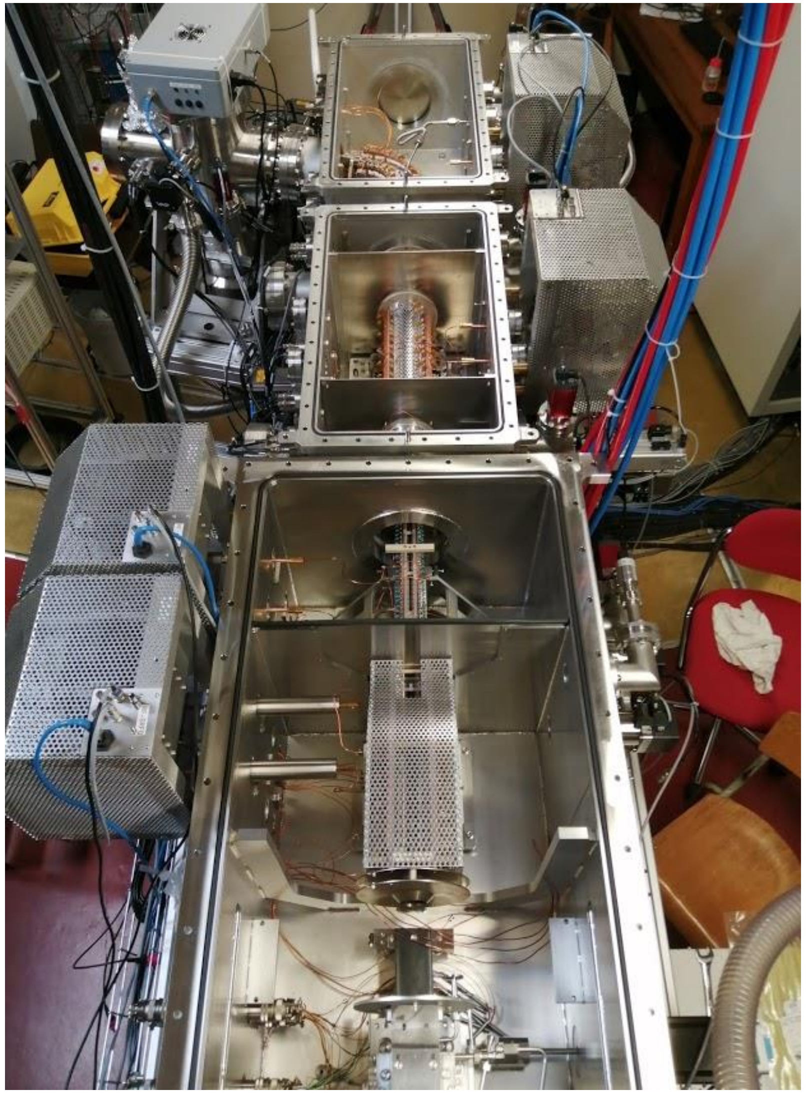

J. Romans, et al., Atoms 10, 21 (2022)
A. Ajayakumar et al., NIMB 539, 102-107 (2023)

Laser system for S³-LEB

- Laser system implemented
  - Gas cell laser ionization: Dual Etalon
  - Gas jet laser ionization: Injection locked laser

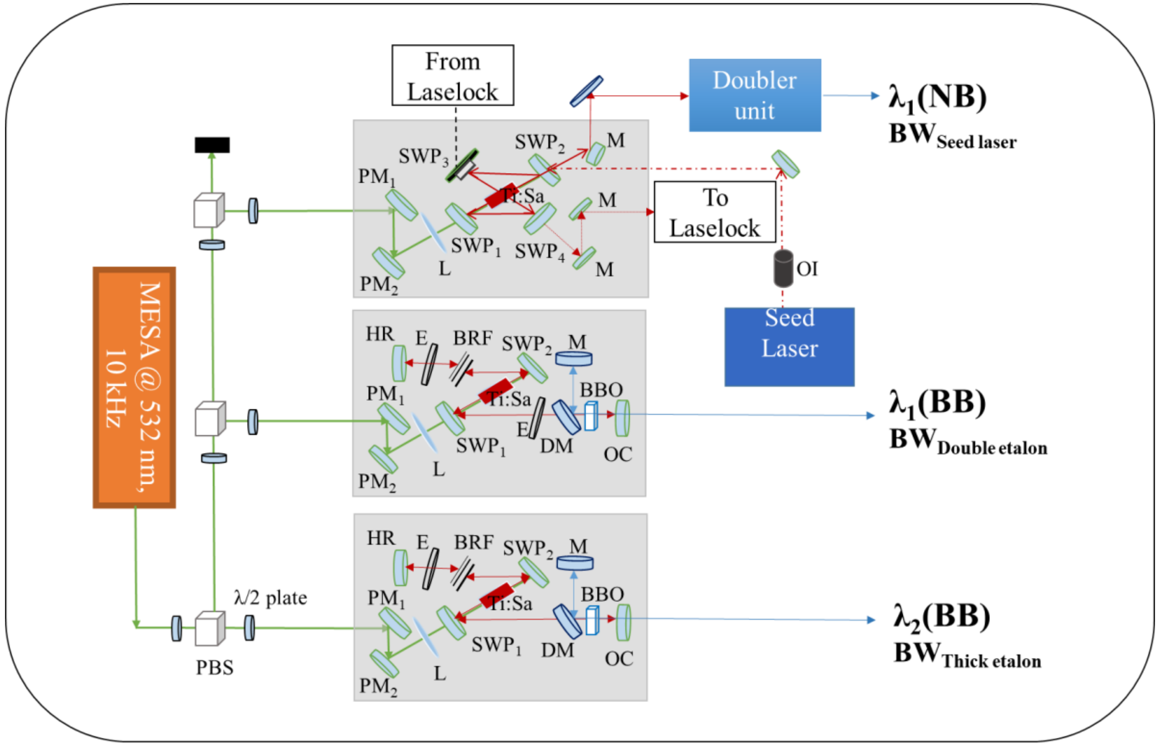

J. Romans et al., NIMB 539, 102–107 (2023)

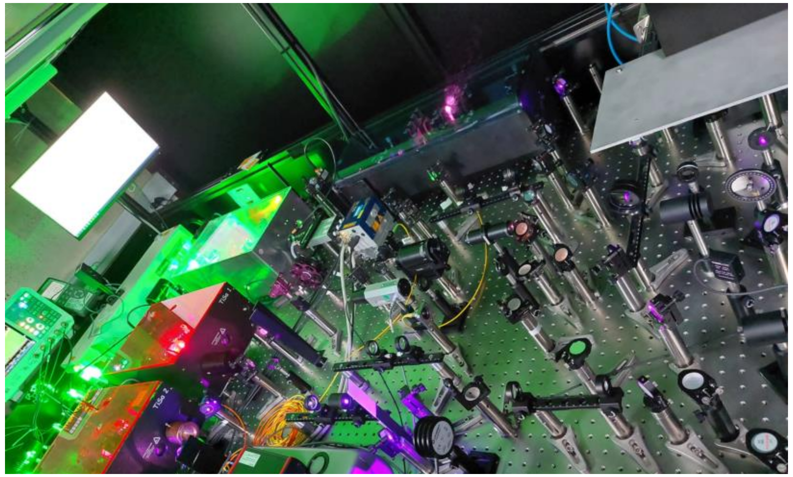

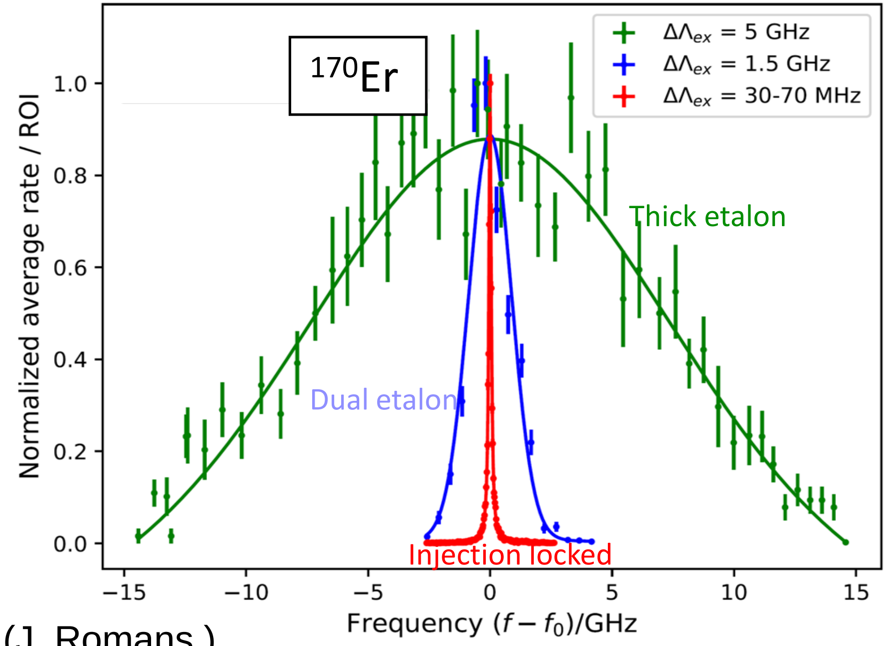

Thesis (J. Romans)

Ion transport towards PILGRIM

Transmission efficiency:

- S-RFQ + miniRFQ: $\epsilon \sim 95(5)\%$
- QMF: $\epsilon \sim 95(5)\%$
- RFQ-CB: $\epsilon_{\text{bunched}} \sim 95(5)\%$
- RFQ-CB – PILGRIM: $\epsilon > 80\%$

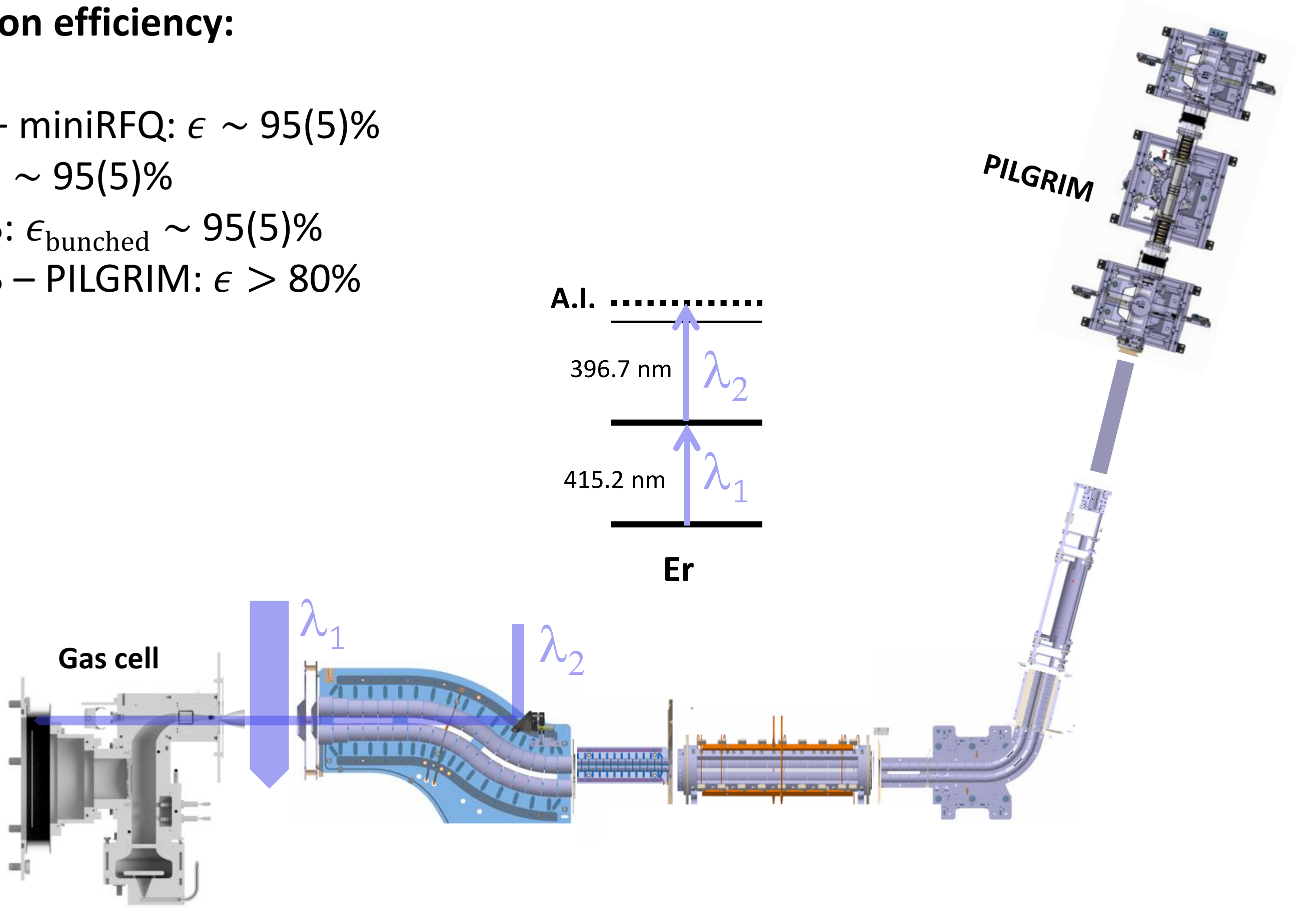

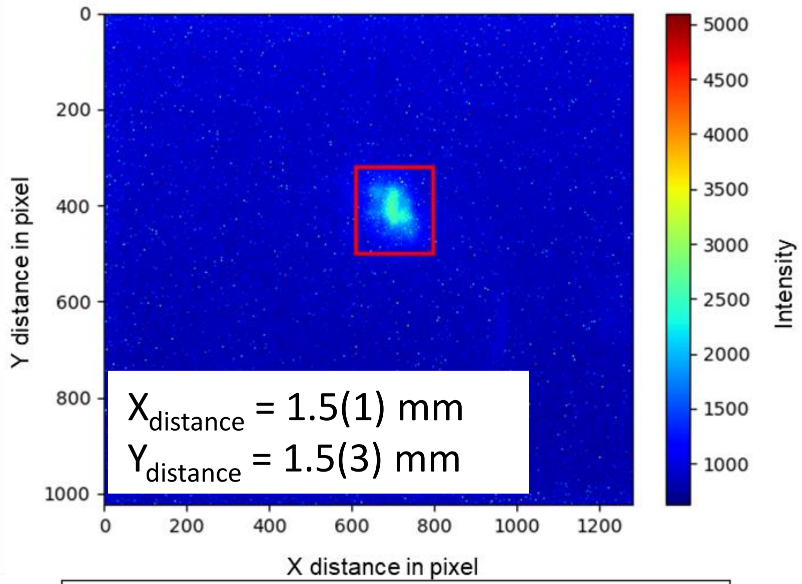

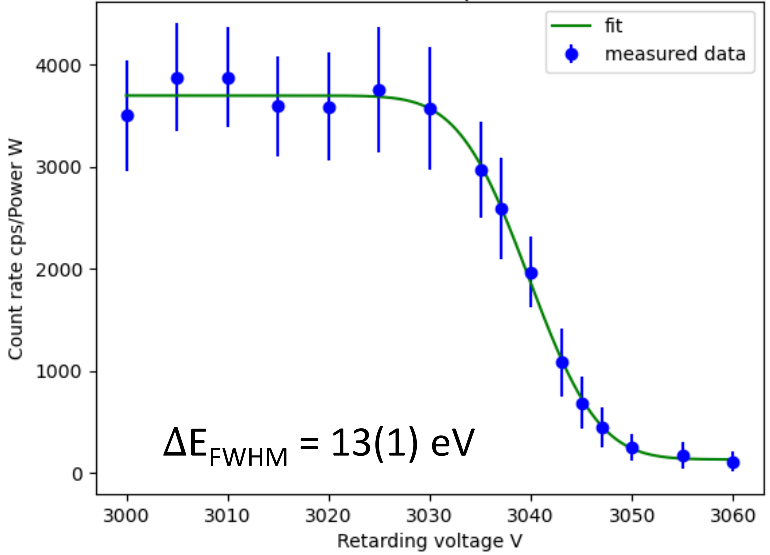

J. Romans, et al., Atoms 10, 21 (2022)
A. Ajayakumar et al., NIMB 539, 102-107 (2023)

Ion transport towards PILGRIM

Transmission efficiency:

- S-RFQ + miniRFQ: $\epsilon \sim 95(5)\%$
- QMF: $\epsilon \sim 95(5)\%$
- RFQ-CB: $\epsilon_{\text{bunched}} \sim 95(5)\%$
- RFQ-CB – PILGRIM: $\epsilon > 80\%$

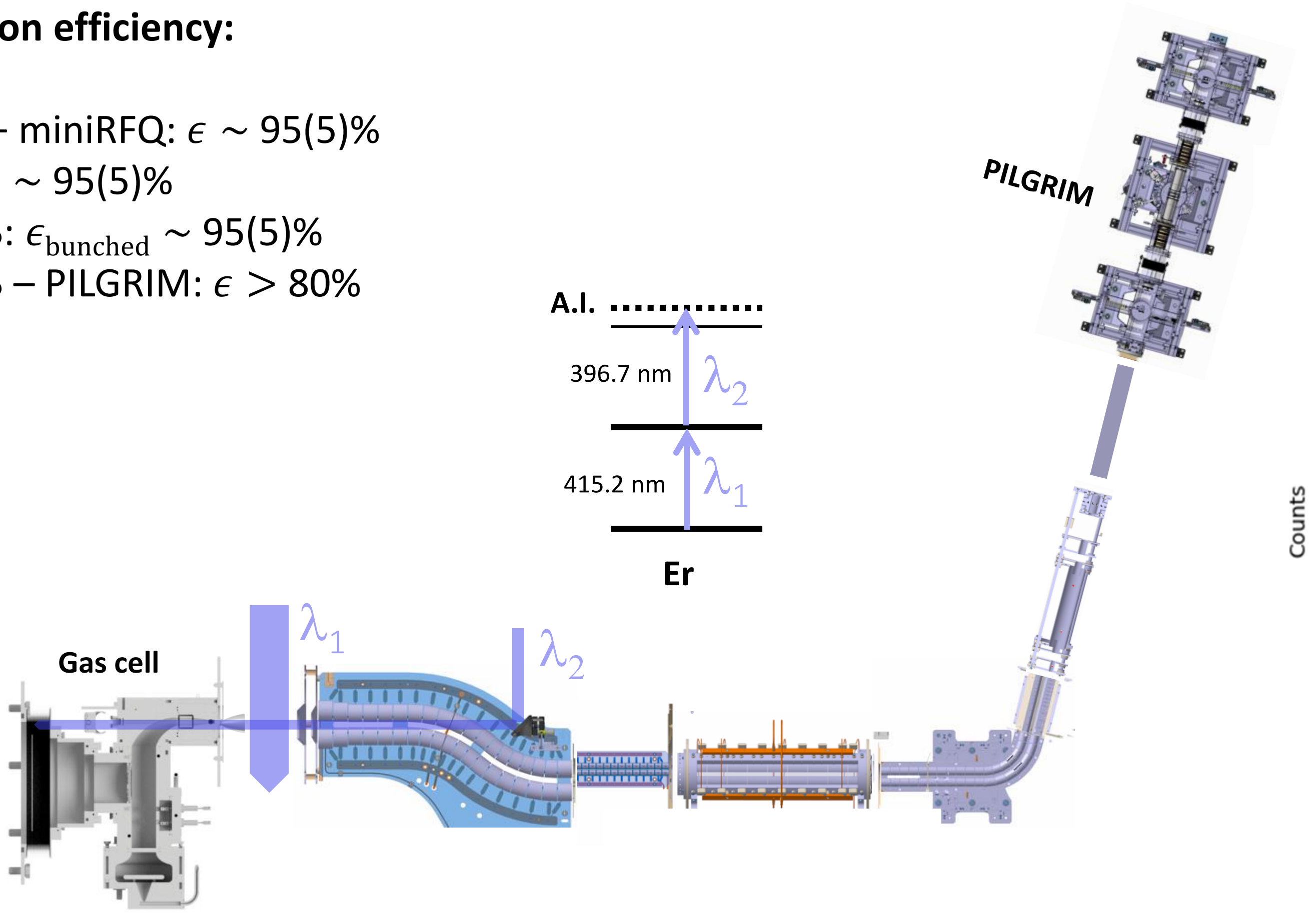

TOF spectra after PILGRIM

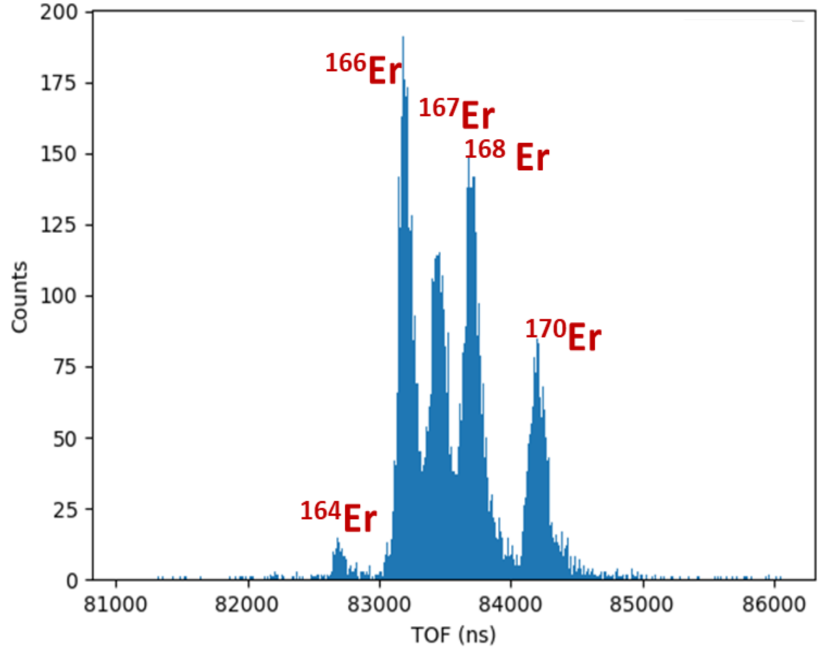

J. Romans, et al., Atoms 10, 21 (2022)
A. Ajayakumar et al., NIMB 539, 102-107 (2023)

PILGRIM: MR-TOF-MS

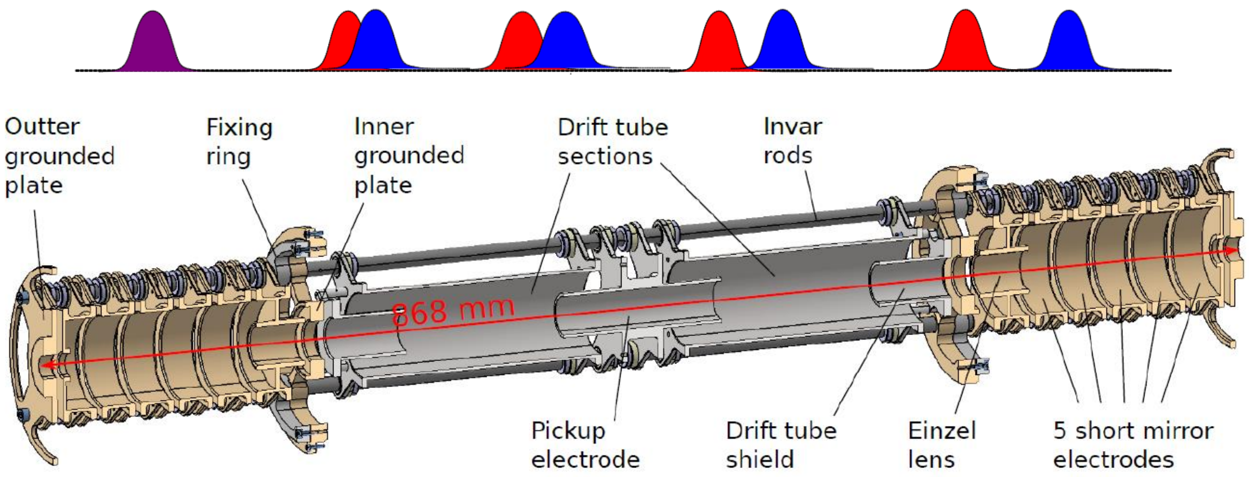

TOF spectra after PILGRIM

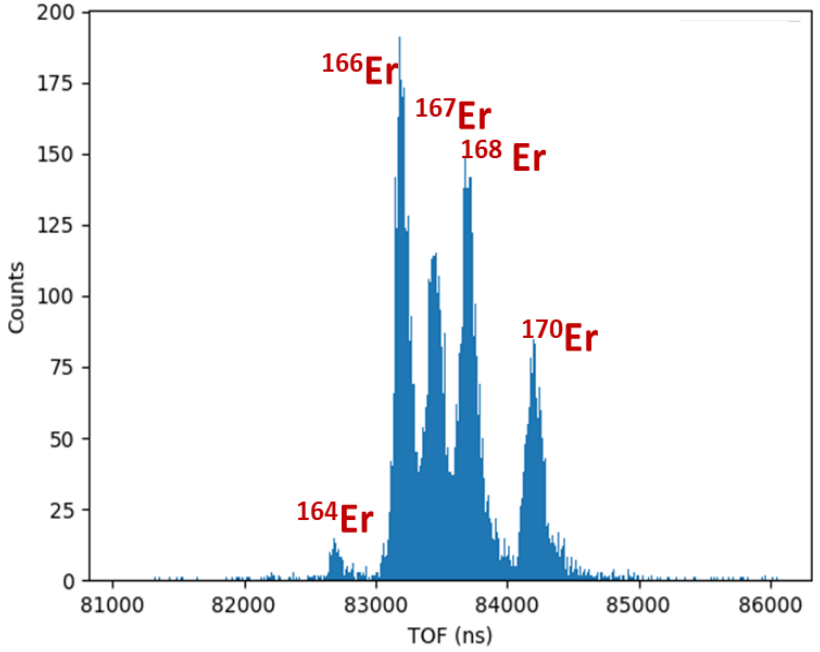

A. Ajayakumar et al., NIMB 539, 102-107 (2023)

Test with ^{170,166,168}Er ions

- R ~ 80000
- Mass accuracy ~ 10^{-7}
- Efficient purification
- Buncher/PILGRIM optimization : R~150000
- Active voltage stabilization optimization to reach R~300000

In-gas cell laser spectroscopy

- Er I Resonance laser ionization
- In gas cell laser ionization
  Dual etalon laser ~ 1.8 GHZ FWHM
- Broadening influences ionization efficiency
- Pressure broadening studies
  Γ_{shift} = -4(1) MHz/mbar
  Γ_{coll} = 11(1) MHz/mbar

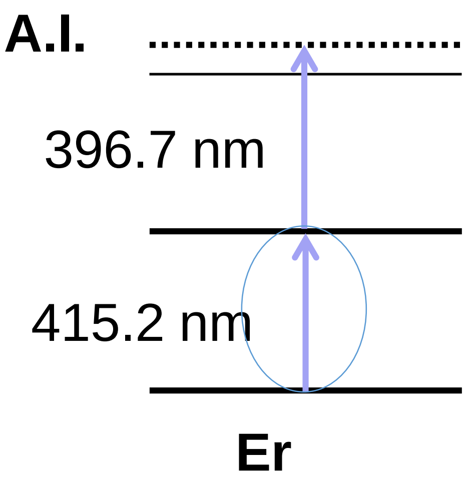

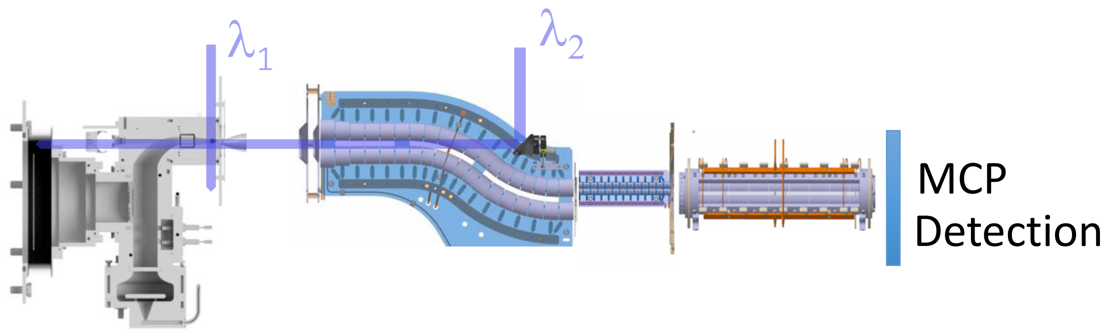

Ar: 200 - 500 mbar

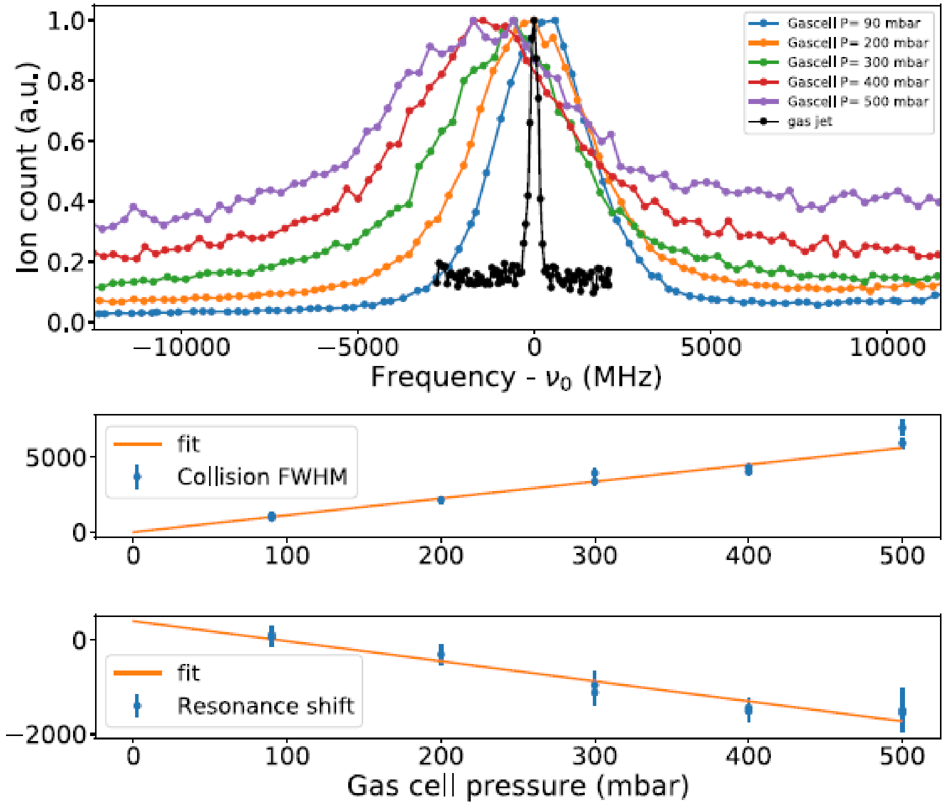

A. Ajayakumar et al., NIMB 539, 102-107 (2023)

In-gas jet laser spectroscopy

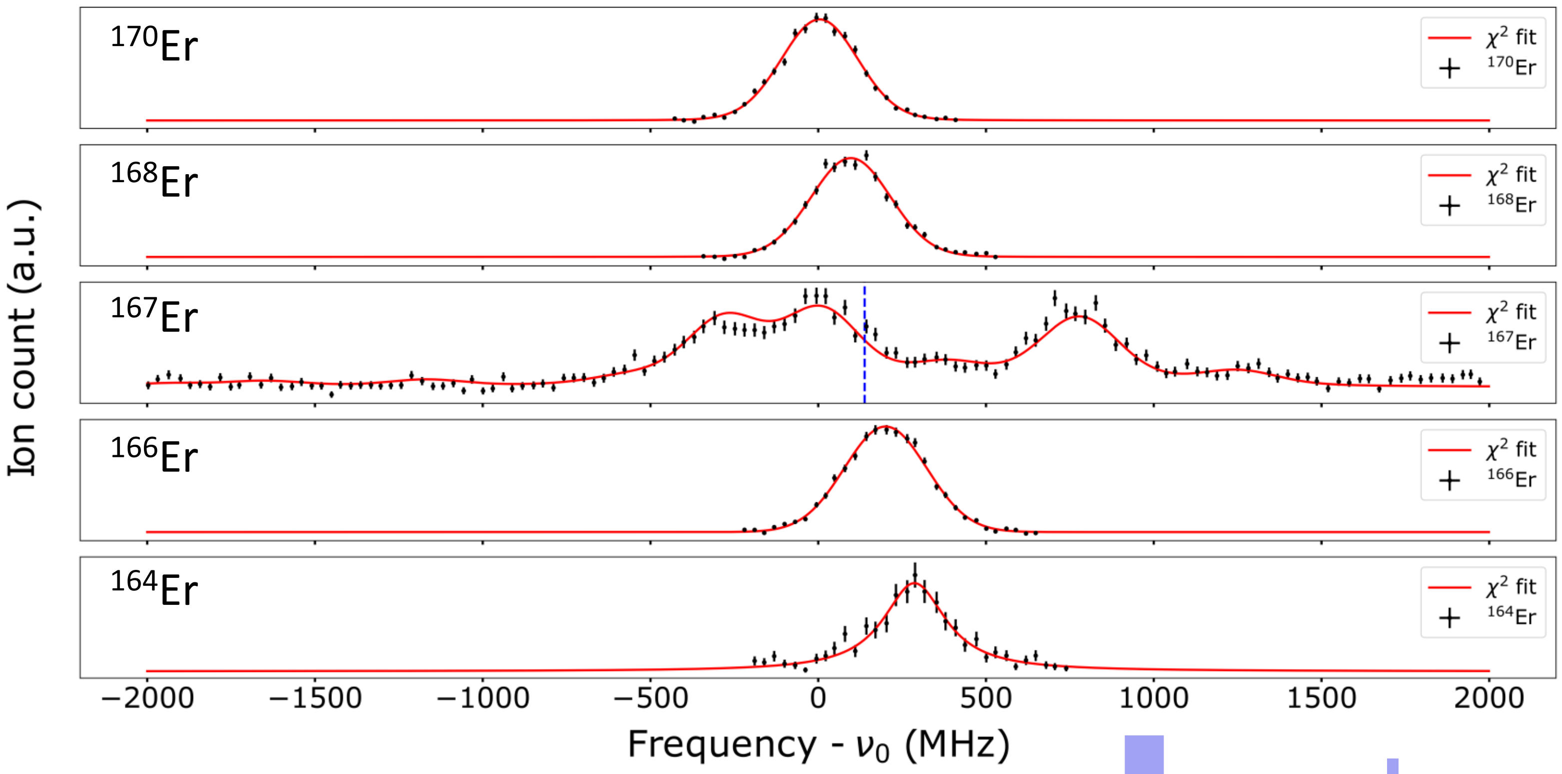

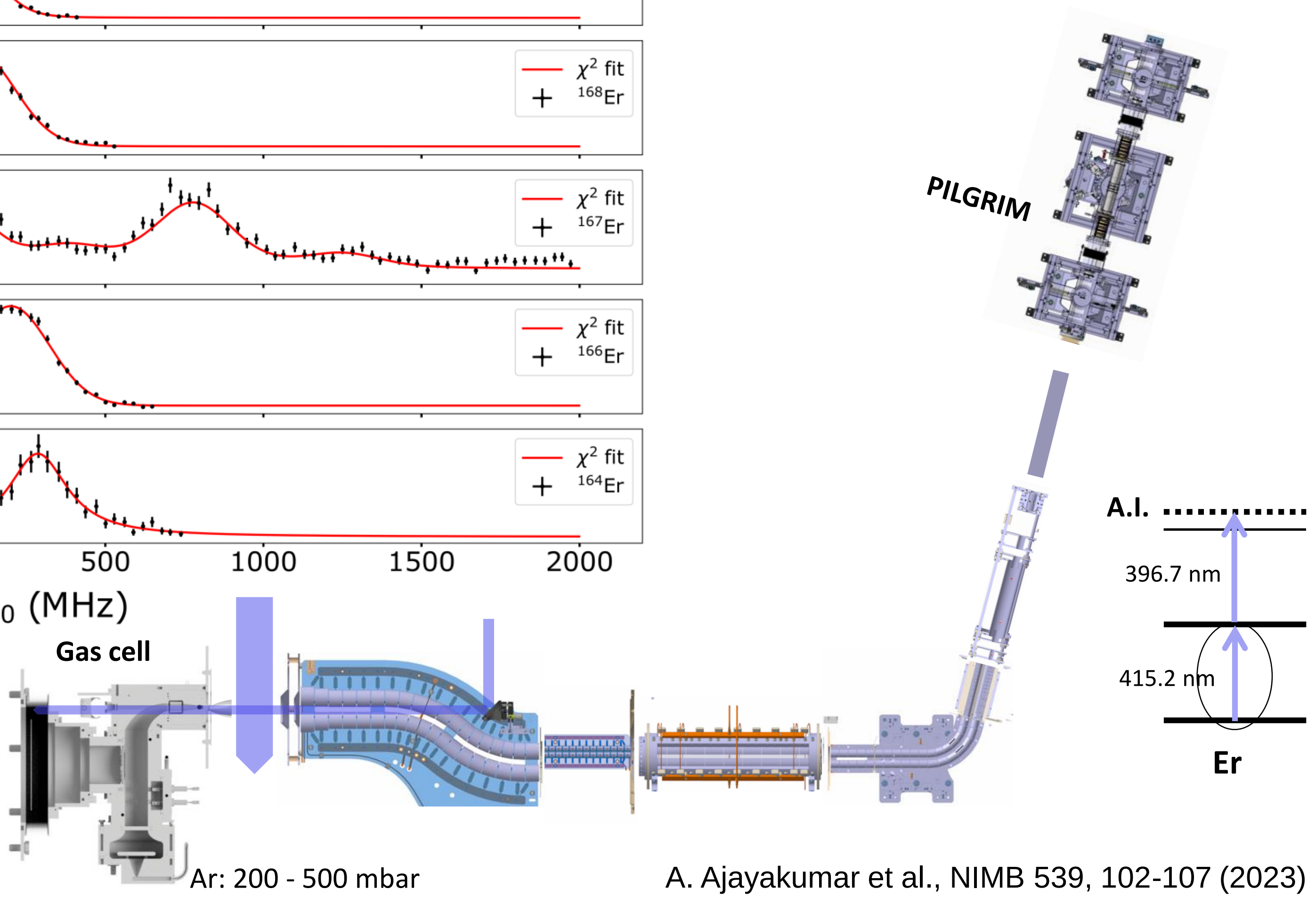

Laser FWHM linewidth ~35 MHz
Spectral FWHM ~ 281(5) MHz

A. Ajayakumar et al., NIMB 539, 102-107 (2023)

In-gas jet laser spectroscopy

- Isotope shift measurement and hyperfine constants
  Agreement with literature

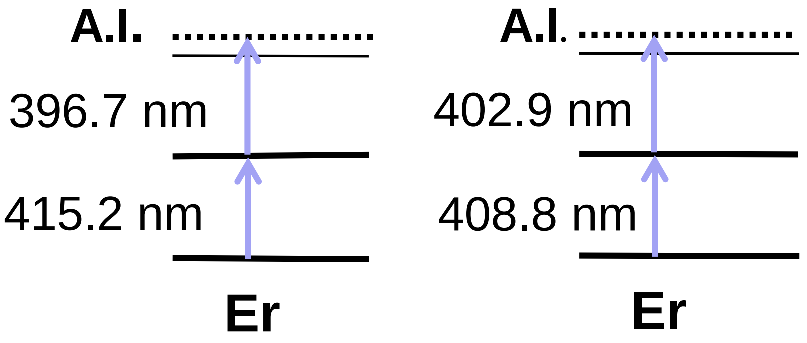

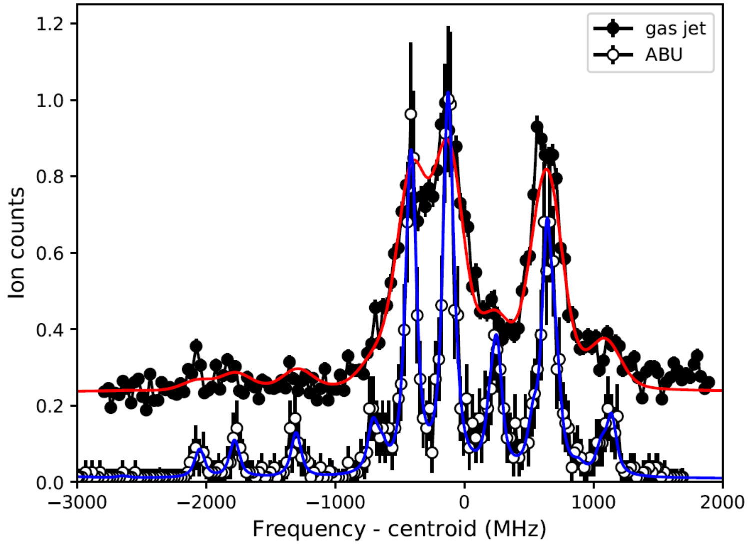

A. Ajayakumar et al., NIMB 539, 102-107 (2023)

$\Delta\nu^{A',170}$ (MHz) $4f^{12}6s^2\ {}^3H_6 \rightarrow 4f^{12}({}^3H)6s6p\ J=5$			^{167}Er HFS coefficients	$4f^{12}6s^2\ {}^3H_6$		$4f^{12}({}^3H_5)6s6p\ J=5$	
Mass number	gas jet	ABU [8]	Method	A (MHz)	B (MHz)	A (MHz)	B (MHz)
168	96(6)	97(8)	gas jet	-122(3)	-4847(237)	-148(4)	-2230(200)
167	138(8)	132(10)	gas jet	-121.8(fixed)	-4563(fixed)	-147.1(7)	-1936(24)
166	196(7)	193(8)	ABU [8]	-121.80(75)	-4563(53)	-147.66(83)	-1888(58)
146	283(7)	298(7)	[28, 29]	-120.487(1)	-4552.984(10)	-146.6(3)	-1874(16)

[8] J. Romans, et al., Nucl. Instrum. Meth. B 536 (2023) 72–81.
[28] W. J. Childs et al., Phys. Rev. A 28 (1983) 3402–3408.
[29] S. Ahmad, et al., Proceedings of the “Symposium on Quantum Electronics” (1985).

In-gas jet laser spectroscopy

- Isotope shift measurements for extraction of charge radii

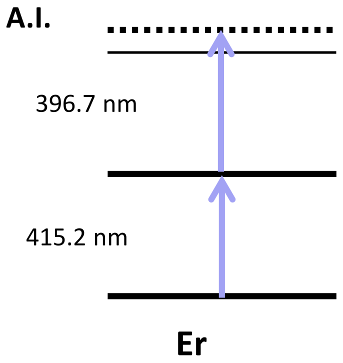

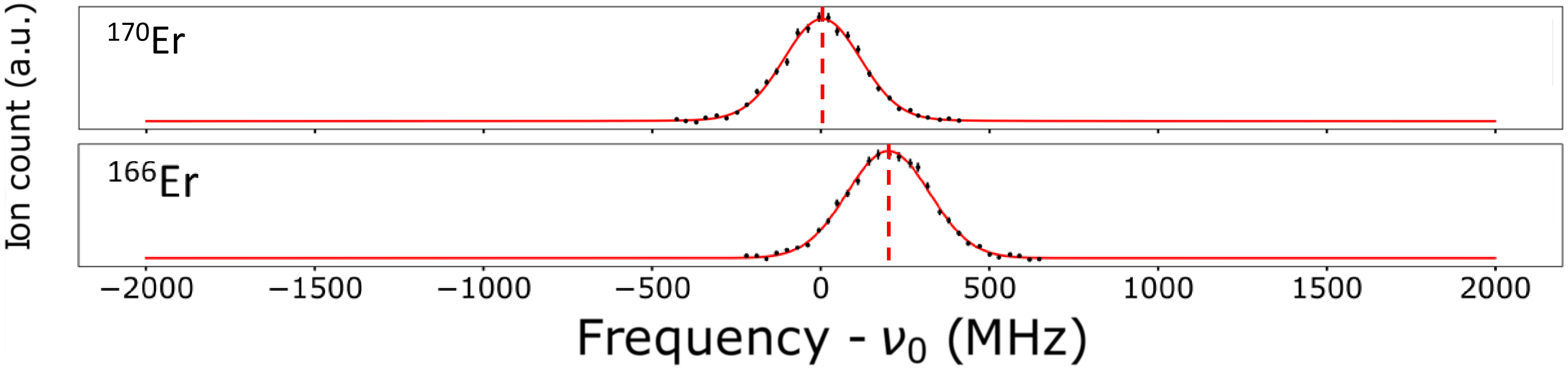

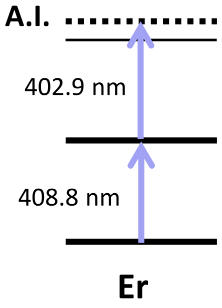

Thesis (W.Dong)

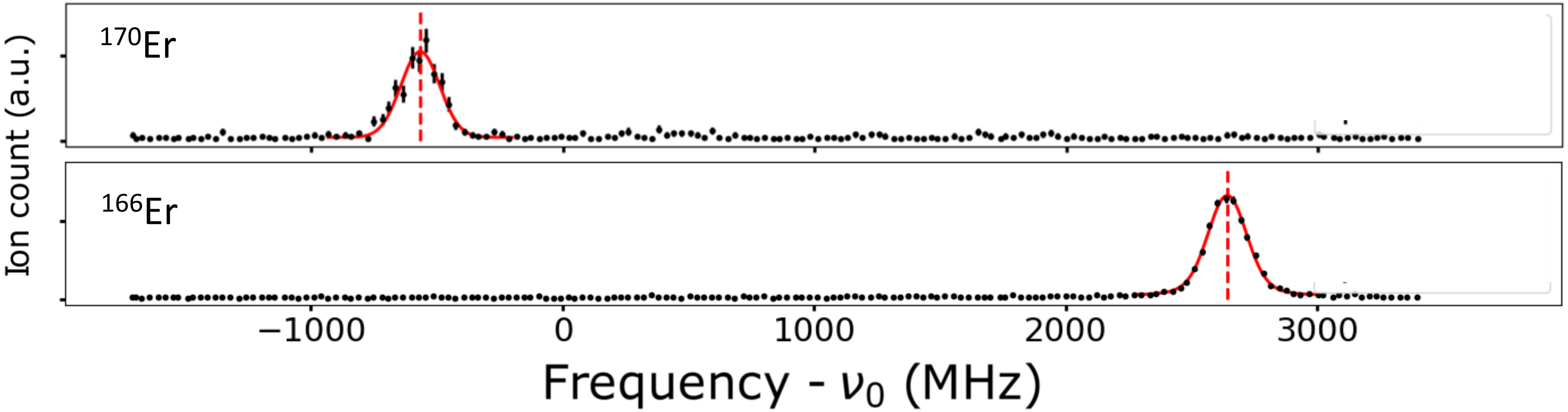

Gas flow characterization

The local temperature of the gas jet:
- Used the transverse first-step laser configuration
- Determined from the Doppler FWHM and atomic transition frequency of the ^{170}Er resonance
- Temperature of the jet T = 46(2) K

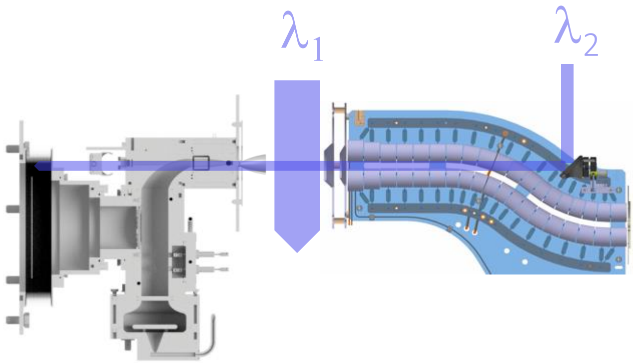

Stream velocity of the jet:
- Used the counter-propagating first-step laser configuration
- Measure Doppler shift
- Stream velocity of the jet u = 565(35) m/s

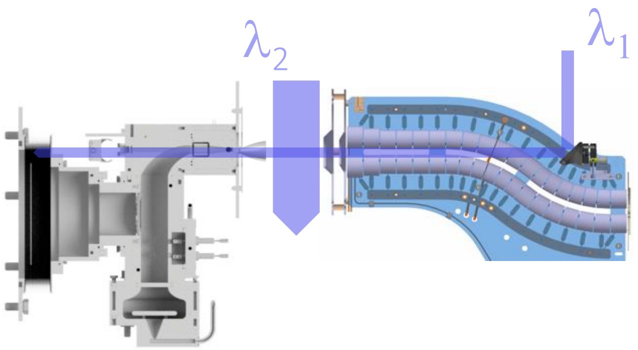

Mach number:
- From the stream velocity (u) and speed of sound, derived from the temperature of the gas jet:
- M = 4.5(3)
- Spectral resolution: 280 MHz

Expected Mach number: 8
Room for improved resolution!

Resonance ionization flow mapping

Possible reasons:

- Flow matching : fine control of P_{cell}/P_{bg}
  under/over expansion
- Power broadening:
  Very efficient transition scheme
- Misalignment of laser

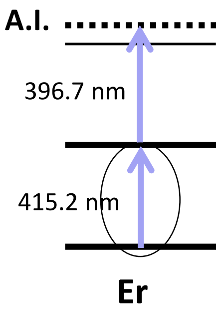

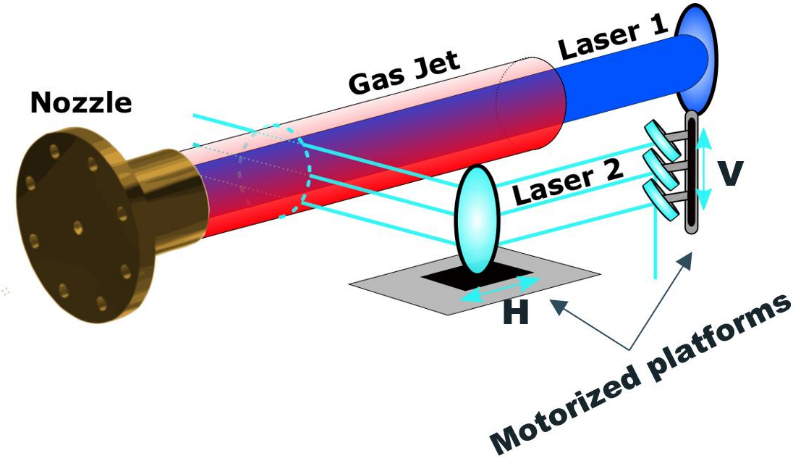

Spectral resolution → 200 MHz

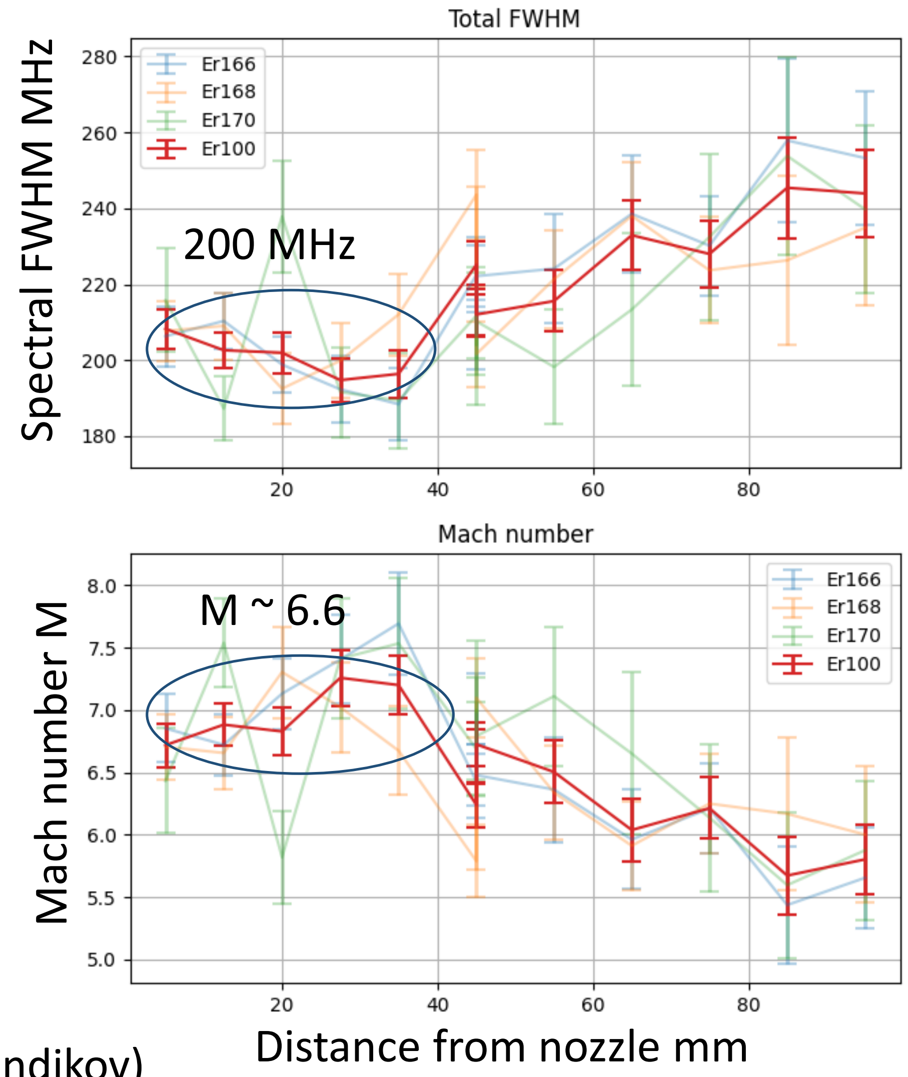

Thesis (F. Ivandikov)

Conclusion

Summary
- In gas-jet laser spectroscopy performed
- Characterization of the gas cell, gas jet
- RFQ Buncher – PILGRIM optimization in progress

Ongoing Technical developments:
- New CW cavity for continuous wavelength scanning
- New Frequency mixing cavity development for extended wavelength range
- Fast gas cell development: ANR FRIENDS3 (IJCLab) (W. Dong)

Installation at S^3
- Installation of S^3-LEB @ S^3 beginning 2024!
- Online commissioning with Er in 2025
- Test of Day 1 experiment elements of interest (Sn, In, Ag, Zr, U…)

S^3-LEB collaboration

GANIL:

Anjali Ajayakumar; Dieter Ackermann; Lucia Caceres; Samuel Damoy; Pierre Delahaye; Patrice Gangnant; Nathalie Lecesne;
Thierry Lefrou; Renan Leroy; Franck Lutton; Alejandro Ortiz;
Benoit Osmond; Julien Piot; Blaise-Maël Retailleau; Hervé Savajols; Gilles Sénécal

LPC:

Frédéric Boumard; Jean-François Cam; Philippe Desrues; Xavier Fléchard; Julien Lory ; Yvan Merrer ; Christophe Vandamme

IJCLab:

Wenling Dong; Patricia Duchesne; Serge Franchoo; Vladimir Manea; Olivier Pochon

KU Leuven:

Arno Claessens; Rafael Ferrer; Mark Huyse; Fedor Ivandikov; Sandro Kraemer ; Yuri Kudriavtsev;
Jekabs Romans; Simon Sels; Paul Van den Bergh; Piet Van Duppen; Matthias Verlinde ; Elise Verstraelen

JGU:

Sebastian Raeder; Dominik Studer; Klaus Wendt

JYU:

Ruben de Groote; Iain David Moore; Michael Reponen; Juha Uusitalo

IPHC:

Emil Traykov

IRFU:

Martial Authier; Olivier Cloue; Antoine Drouard; Thomas Goigoux;
Emmanuel Rey-Herme; Damien Thisse; Marine Vandebrouck

and the RESIST network in ENSAR2

Supersonic gas jet

- Mach number: $M = \frac{v_{jet}}{v_{sound@jet}}$

- Super/hypersonic jet = cold jet → low Doppler broadening

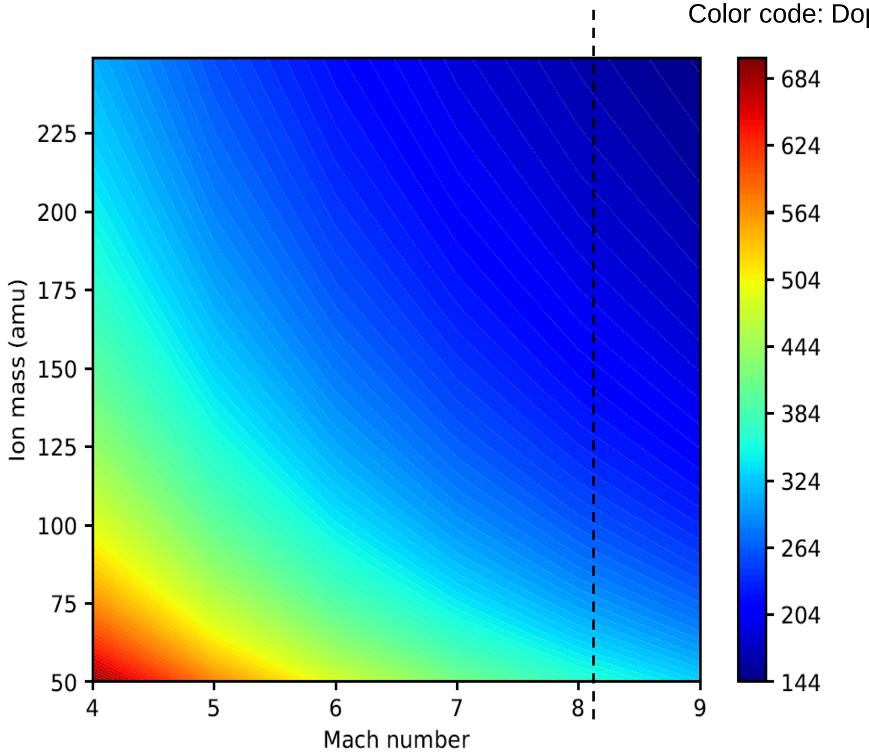

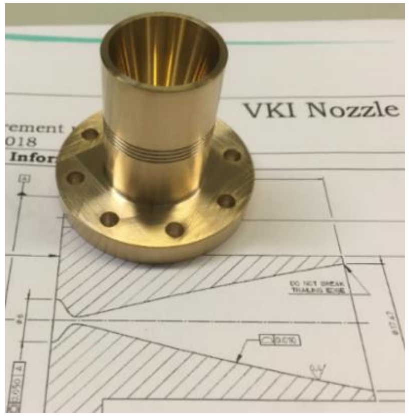

M = 8.1 de Laval nozzle

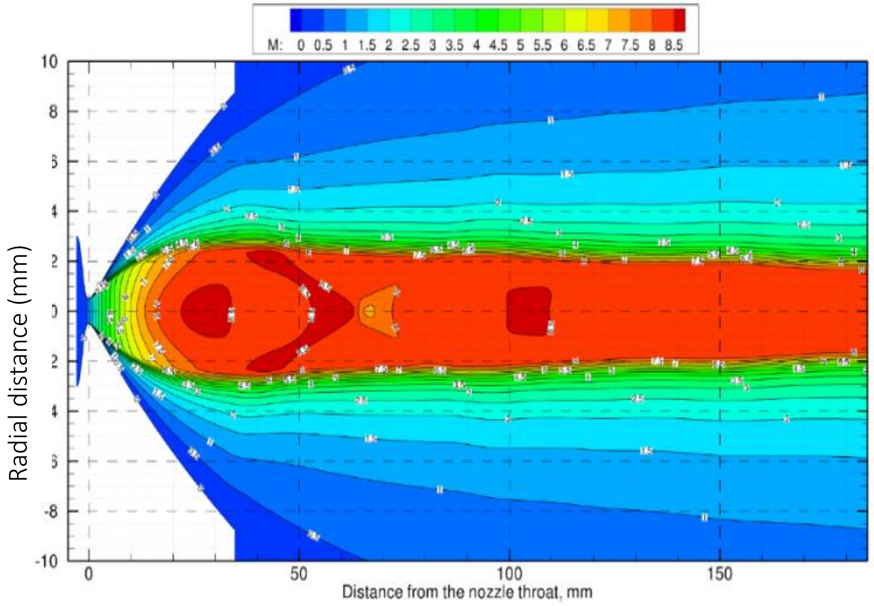

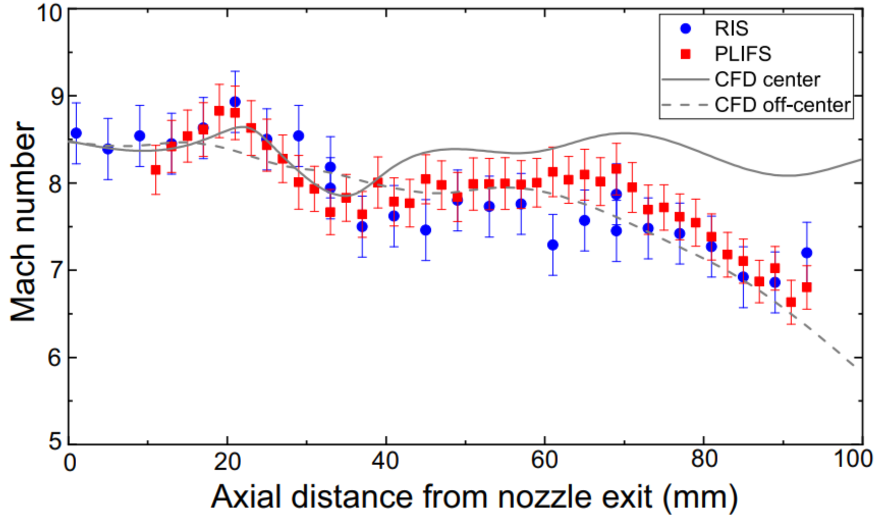

Nuclear information

- Exploits the hyperfine interaction to extract nuclear observables

- coupling of nuclear spin and electronic angular momentum results

Hyperfine parameters

$$W_F = \frac{1}{2}AC + B\frac{\frac{3}{4}C(C+1) - I(I+1)J(J+1)}{2I(2I-1)J(2J-1)}$$

$$C = F(F+1) - I(I+1) - J(J+1)$$

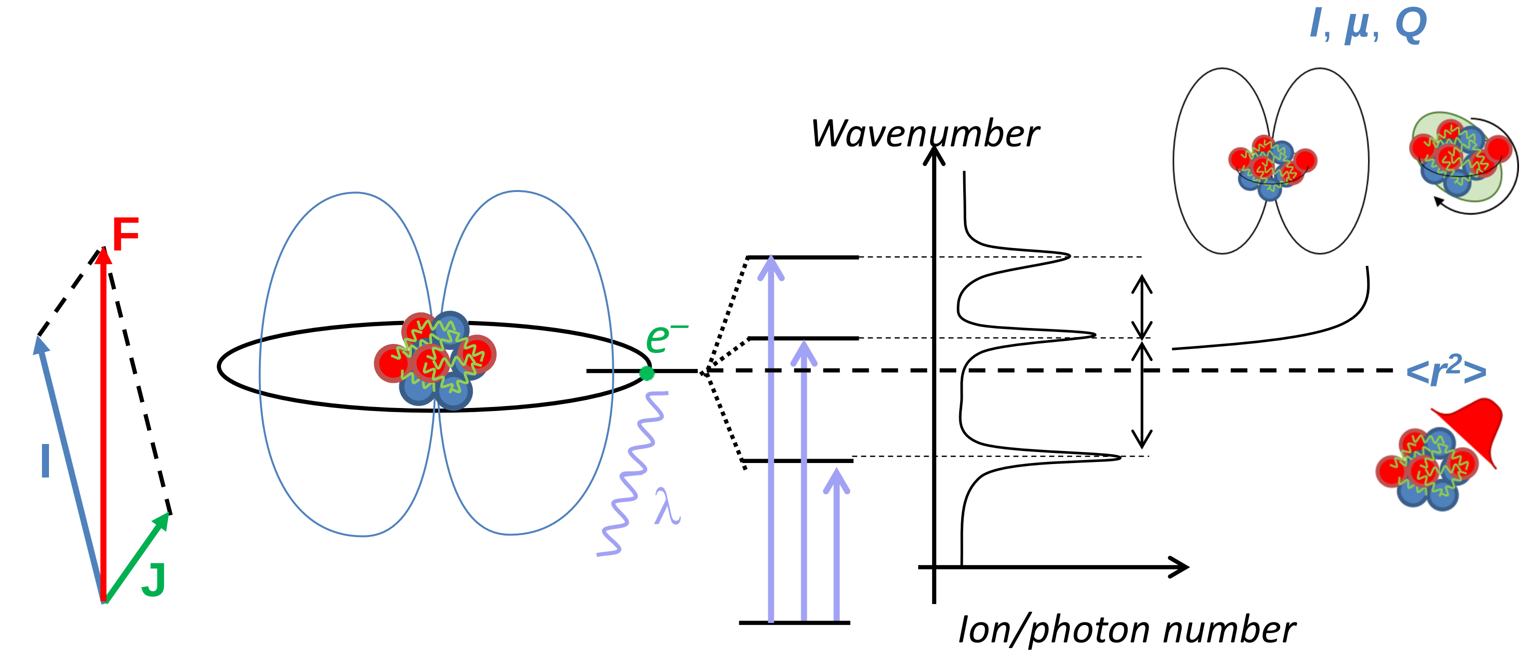

$$\frac{A}{A'} = \frac{\mu}{\mu'}\frac{I'}{I}$$

$$\frac{B}{B'} = \frac{Q_s}{Q'_s}$$

Isotope shift

$$\delta\nu_i^{AA'} = M_i\frac{m'_A - m_A}{m'_A m_A} + F_i\delta\langle r^2\rangle^{A,A'}$$

$$\delta\nu_{MS}^{AA'} = (K_{NMS} + K_{SMS})\frac{m_{A'} - m_A}{m_{A'}m_A} = M\frac{m_{A'} - m_A}{m_{A'}m_A}$$

K_{NMS} → $(m_e/m_p)\upsilon_0$

Erbium commissoning

^{152}Er
z: 68 n: 84
Jπ: 0+
$T_{1/2}$:10.3 s 0.1
decay α 90%
ec β+ 10%

150 Er	151 Er	152 Er	153 Er	154 Er
9	9	8	8	6
2.36e+4	1.42e+5	1.96e+4	1.52e+1	1.28e-3
8.925%	10.129%	11.13%	11.827%	12.941%

IS measurement

$$\delta\nu_{MS}^{AA'} = (K_{NMS} + K_{SMS})\frac{m_{A'} - m_A}{m_{A'} m_A} = M\frac{m_{A'} - m_A}{m_{A'} m_A}$$

$$\mu^{A,A'}\delta\nu_i^{AA'} = M_i + F_i\mu^{A,A'}\delta\langle r^2\rangle^{A,A'}$$

M and F factor – atomic factor describing mass and field shift

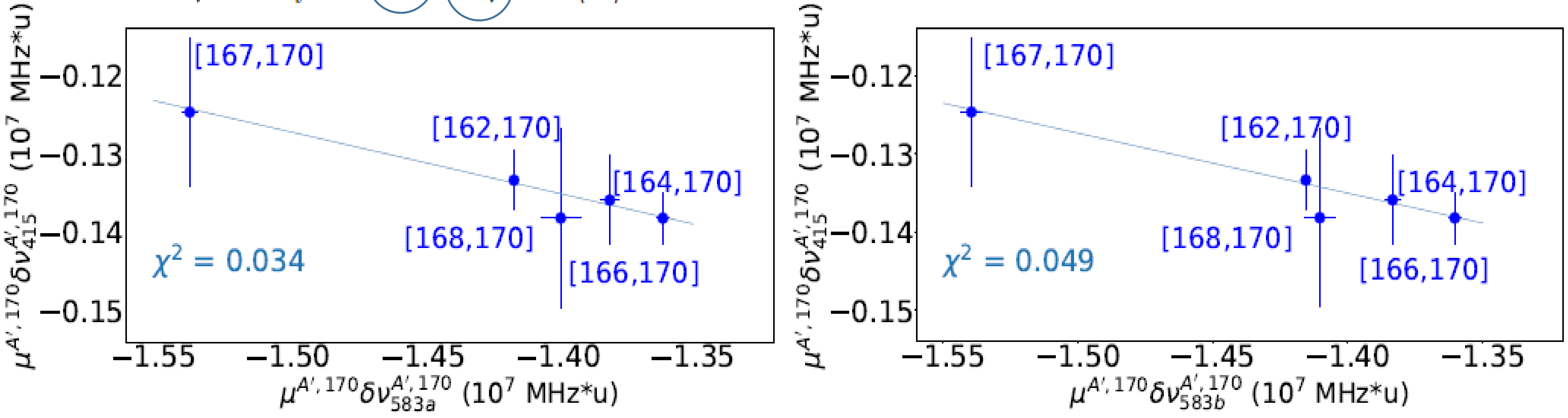

Ref.$_{IS}$	Ref.$_{muon}$	Ref.$_{F\&M}$	F_{415} (MHz fm^{-2})	M_{415} (GHz u)
[103][a]		[51, 62][a]	636(77)	-2474(197)
[109][b]		[109][b]	514(77)	-2445(213)
	[109][c]		469(322)	-2352(698)

Atomic transition is not very sensitive to changes in δ <r^2>

Doppler FWHM

$$\Delta\nu_{\text{Doppler}} = 2\sqrt{\ln 2}\,\frac{\nu_{01}}{c}\sqrt{\frac{2kT}{m}}$$

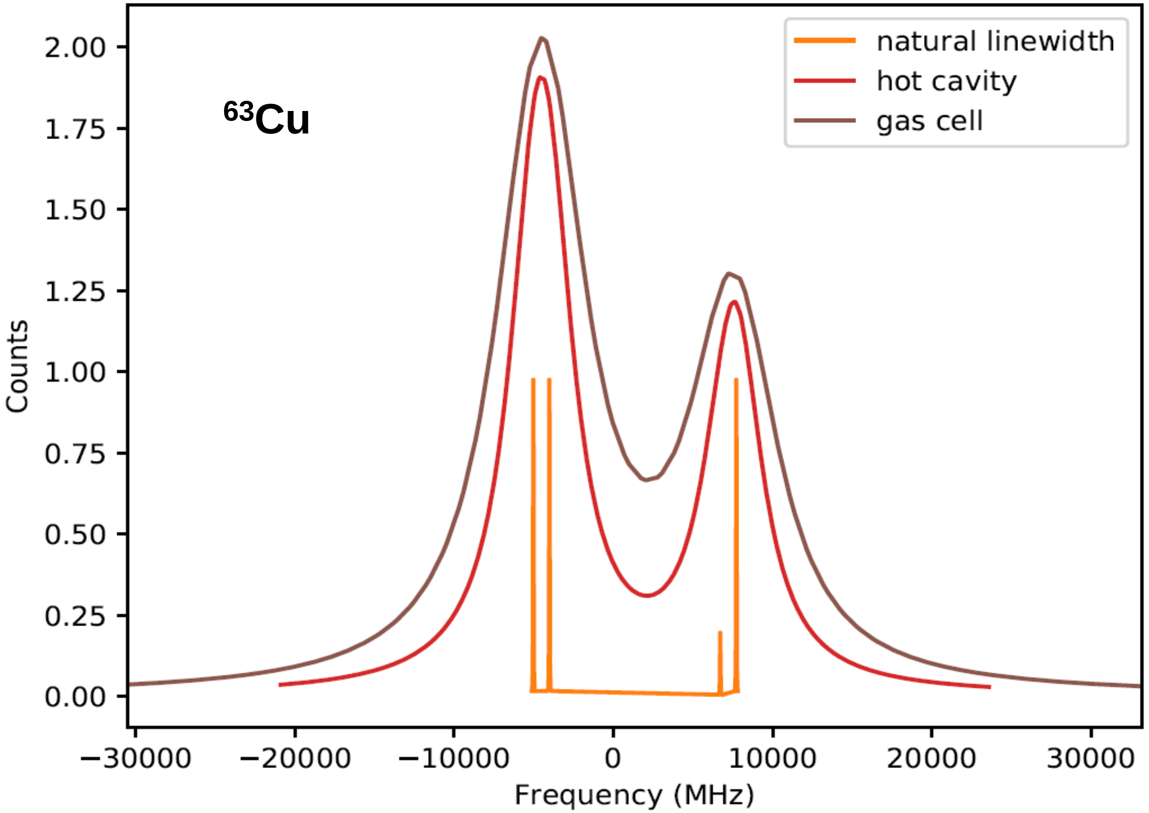

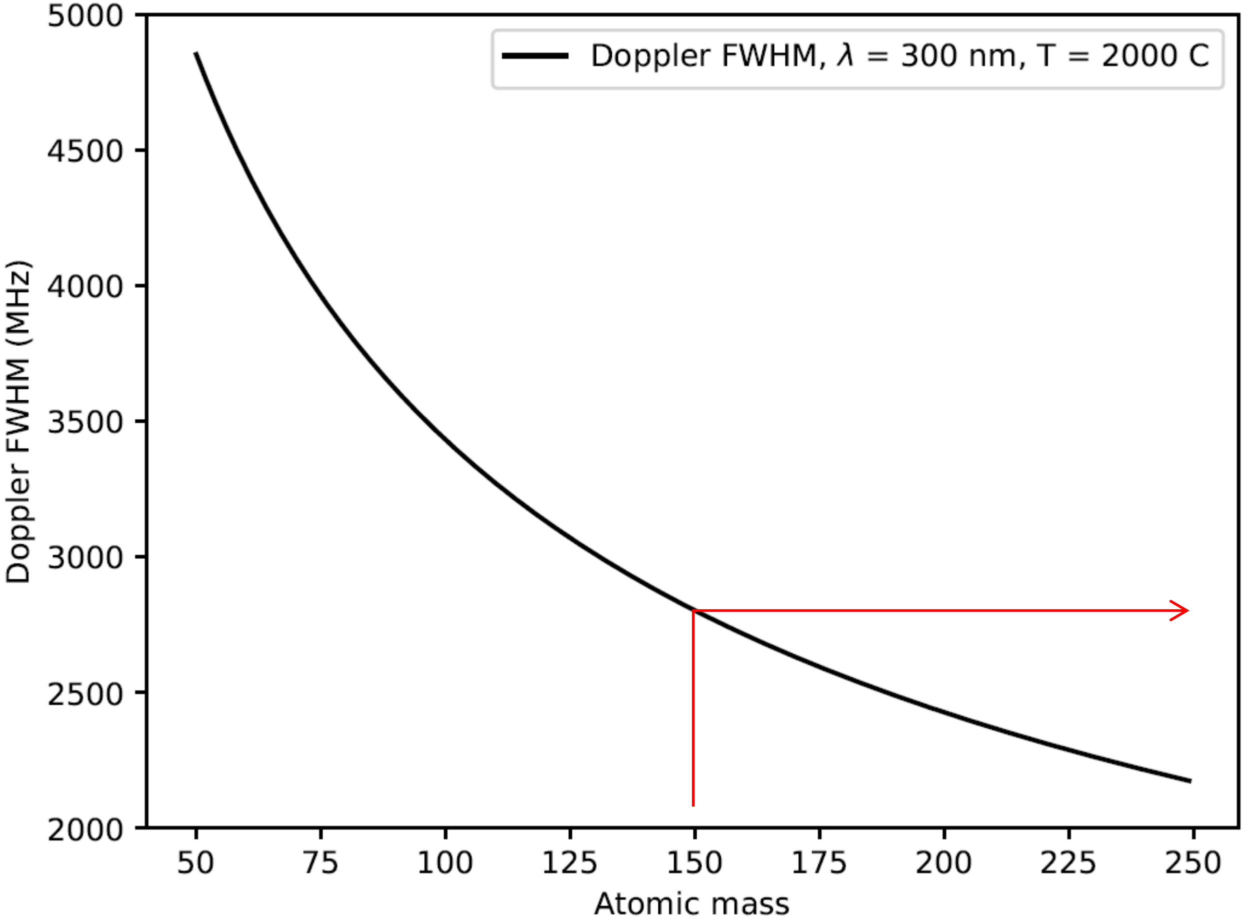

V. N. Fedosseev et al., Phys. Scr. **85**, 058104 (2012)

Pressure FWHM

$$L(\nu - \nu_{01}) = \frac{1}{2\pi} \frac{\Gamma}{(\nu - \nu_{01} + \Gamma_{sh})^2 + (\Gamma/2)^2},$$

$$\Gamma = \Gamma_{nat} + \Gamma_{coll}$$

$$\Gamma_{coll} = \gamma_{coll} \cdot \rho$$

$$\Gamma_{sh} = \gamma_{sh} \cdot \rho,$$

In-gas laser ionization and spectroscopy of $^{210-213}$Ac and 213,215Th

Spokesperson: R.Ferrer

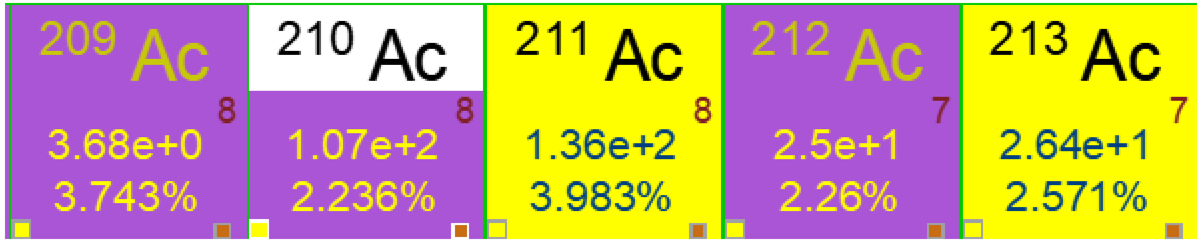

Measure ground state properties using isotope shifts and hyperfine structure

Isotope	Photo-ions (pps)	Counts(pps)	Scan time
^{215}Th	4	1.6	2 h
^{213}Th	0.05	0.02	6.3 d
$^{212+213}$Ac	9	3.6	1 h
$^{210+211}$Ac	6	2.4	1.3 h

Mass measurements and laser spectroscopy around ^{100}Sn

In-jet resonance ionisation spectroscopy to measure the hyperfine structure splittings and isotope shifts in atomic transitions for the Sn isotopes A = 101-105.

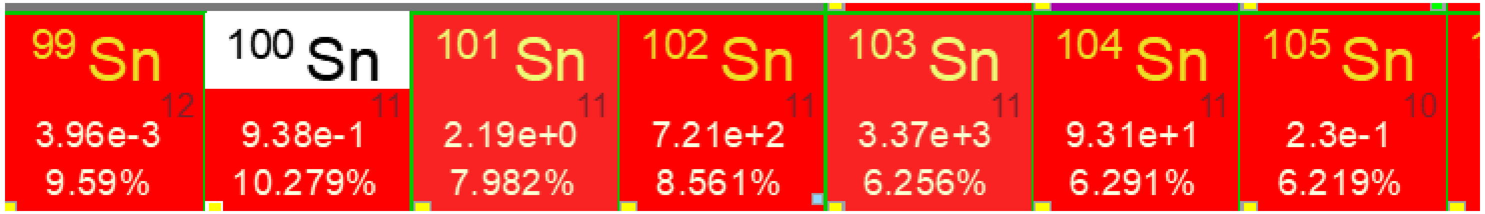

Measurement of ground-state properties to study the evolution of nuclear structure properties approaching the N=Z=50 shell closures.

Mass measurements and laser spectroscopy of n-deficient isotopes in the A ~ 80 region of deformation

Spokesperson: **P. Ascher (masses) and S. Grévy (laser spectroscopy)**

^{77}Zr	^{78}Zr	^{79}Zr	^{80}Zr
10	9	9	3
2.27e-4	2.46e-5	1.66e-6	7.05e-10
3.012%	5.076%	5.451%	7.548%

^{36}Ar-^{50}Cr

-extend measurements to the more neutron deficient isotopes of Zr towards the doubly closed shell 80Zr and to the neighboring nuclei

Search for octupole deformation in 225-228U

Spokesperson: M. Vandebrouck

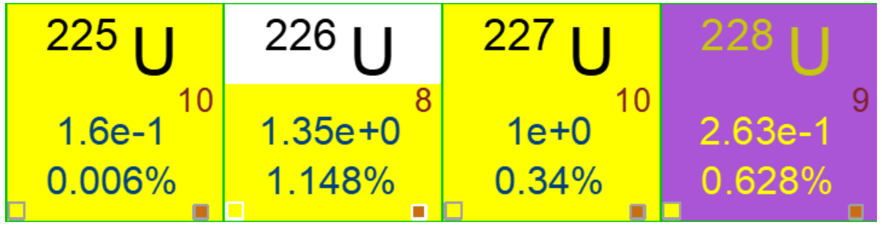

Information limited to 233-238 U

$^{208}Pb(^{22}Ne, xn)^{230-x}$ U

Reaction	Beam energy [MeV]	Cross-section [μb]	Counting rate (LEB Detector) [pps]
$^{208}Pb(^{22}Ne, 5n)^{225}U$	116	2	0.9
$^{208}Pb(^{22}Ne, 4n)^{226}U$	108	6	2.7
$^{208}Pb(^{22}Ne, 3n)^{227}U$	106	10	4.5
$^{208}Pb(^{22}Ne, 2n)^{228}U$	97	2	0.9

LOI

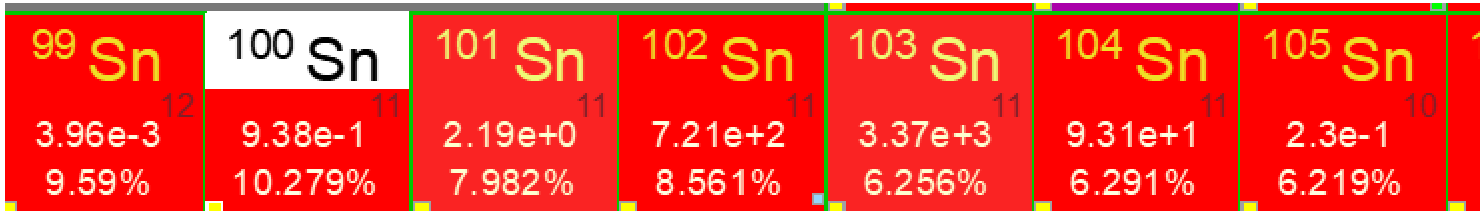
99 Sn
12
3.96e-3
9.59%
100 Sn
11
9.38e-1
10.279%
101 Sn
11
2.19e+0
7.982%
102 Sn
11
7.21e+2
8.561%
103 Sn
11
3.37e+3
6.256%
104 Sn
11
9.31e+1
6.291%
105 Sn
10
2.3e-1
6.219%

LOI

^{99}Sn	^{100}Sn	^{101}Sn	^{102}Sn	^{103}Sn	^{104}Sn	^{105}Sn
12	11	11	11	11	11	10
3.96e-3	9.38e-1	2.19e+0	7.21e+2	3.37e+3	9.31e+1	2.3e-1
9.59%	10.279%	7.982%	8.561%	6.256%	6.291%	6.219%

^{209}Ac	^{210}Ac	^{211}Ac	^{212}Ac	^{213}Ac
8	8	8	7	7
3.68e+0	1.07e+2	1.36e+2	2.5e+1	2.64e+1
3.743%	2.236%	3.983%	2.26%	2.571%

^{77}Zr	^{78}Zr	^{79}Zr	^{80}Zr
10	9	9	3
2.27e-4	2.46e-5	1.66e-6	7.05e-10
3.012%	5.076%	5.451%	7.548%

^{225}U	^{226}U	^{227}U	^{228}U
10	8	10	9
1.6e-1	1.35e+0	1e+0	2.63e-1
0.006%	1.148%	0.34%	0.628%